NAVAL POSTGRADUATE SCHOOL

MONTEREY, CALIFORNIA

THESIS

OBSERVATION OF PASSIVE BROADBAND SUPPRESSION OF LOW-FREQUENCY UNDERWATER SOUND

by

Evan J. McMellon

December 2020

Thesis Advisor: Bruce C. Denardo
Co-Advisor: Oleg A. Godin

THIS PAGE INTENTIONALLY LEFT BLANK

REPORT DOCUMENTATION PAGE			*Form Approved OMB No. 0704-0188*

1. AGENCY USE ONLY *(Leave blank)*	**2. REPORT DATE** December 2020	**3. REPORT TYPE AND DATES COVERED** Master's thesis

4. TITLE AND SUBTITLE
OBSERVATION OF PASSIVE BROADBAND SUPPRESSION OF LOW-FREQUENCY UNDERWATER SOUND

5. FUNDING NUMBERS

6. AUTHOR(S) Evan J. McMellon

7. PERFORMING ORGANIZATION NAME(S) AND ADDRESS(ES)
Naval Postgraduate School
Monterey, CA 93943-5000

8. PERFORMING ORGANIZATION REPORT NUMBER

9. SPONSORING / MONITORING AGENCY NAME(S) AND ADDRESS(ES)
N/A

10. SPONSORING / MONITORING AGENCY REPORT NUMBER

11. SUPPLEMENTARY NOTES The views expressed in this thesis are those of the author and do not reflect the official policy or position of the Department of Defense or the U.S. Government.

12a. DISTRIBUTION / AVAILABILITY STATEMENT
Approved for public release. Distribution is unlimited.

12b. DISTRIBUTION CODE
A

13. ABSTRACT (maximum 200 words)

We develop a proof-of-principle experiment for a recent theory published by Godin and Baynes, who showed that passive, broadband suppression of underwater sound can occur when a balloon or bladder filled with air is near a low-frequency sound source. The volume of air produces a pressure-release boundary condition that causes scattering, which redirects energy and can destructively interfere with the direct sound from the source. One application of this effect is in Naval vessels, which emit low-frequency sound due to cavitation and vibrations and can thus be acoustically detected. However, it may be that the sound can be significantly reduced with the simple use of a bladder on the hull of the vessel. Experiments with and without a balloon filled with air in the presence of a sound source were conducted in the NPS tank laboratory in Spanagel Hall. Quantitative comparison with the theory indicates agreement, but the results are only rough due to reflections from the surfaces of the water in the tank. We were unable to gate the signal in order to avoid the reflected sound for our experimental parameter values, which were chosen for optimal sound suppression according to the theory. Future experimentation will be conducted in the NPS SLAMR facility, which should be sufficiently deep and wide to allow for the use of gating.

14. SUBJECT TERMS
noise suppression

15. NUMBER OF PAGES
69

16. PRICE CODE

17. SECURITY CLASSIFICATION OF REPORT	**18. SECURITY CLASSIFICATION OF THIS PAGE**	**19. SECURITY CLASSIFICATION OF ABSTRACT**	**20. LIMITATION OF ABSTRACT**
Unclassified	Unclassified	Unclassified	UU

NSN 7540-01-280-5500

Standard Form 298 (Rev. 2-89)
Prescribed by ANSI Std. 239-18

THIS PAGE INTENTIONALLY LEFT BLANK

Approved for public release. Distribution is unlimited.

OBSERVATION OF PASSIVE BROADBAND SUPPRESSION OF LOW-FREQUENCY UNDERWATER SOUND

Evan J. McMellon
Ensign, United States Navy
BS, North Carolina State University, 2019

Submitted in partial fulfillment of the
requirements for the degree of

MASTER OF SCIENCE IN ENGINEERING ACOUSTICS

from the

NAVAL POSTGRADUATE SCHOOL
December 2020

Approved by: Bruce C. Denardo
Advisor

Oleg A. Godin
Co-Advisor

Oleg A. Godin
Chair, Department of Physics

THIS PAGE INTENTIONALLY LEFT BLANK

ABSTRACT

We develop a proof-of-principle experiment for a recent theory published by Godin and Baynes, who showed that passive, broadband suppression of underwater sound can occur when a balloon or bladder filled with air is near a low-frequency sound source. The volume of air produces a pressure-release boundary condition that causes scattering, which redirects energy and can destructively interfere with the direct sound from the source. One application of this effect is in Naval vessels, which emit low-frequency sound due to cavitation and vibrations and can thus be acoustically detected. However, it may be that the sound can be significantly reduced with the simple use of a bladder on the hull of the vessel. Experiments with and without a balloon filled with air in the presence of a sound source were conducted in the NPS tank laboratory in Spanagel Hall. Quantitative comparison with the theory indicates agreement, but the results are only rough due to reflections from the surfaces of the water in the tank. We were unable to gate the signal in order to avoid the reflected sound for our experimental parameter values, which were chosen for optimal sound suppression according to the theory. Future experimentation will be conducted in the NPS SLAMR facility, which should be sufficiently deep and wide to allow for the use of gating.

THIS PAGE INTENTIONALLY LEFT BLANK

TABLE OF CONTENTS

THIS PAGE INTENTIONALLY LEFT BLANK

LIST OF FIGURES

LIST OF TABLES

THIS PAGE INTENTIONALLY LEFT BLANK

ACKNOWLEDGMENTS

I would like to thank my amazing parents for the opportunities they have created for me and the encouragement and support they provide. I would also like to thank my girlfriend, McKenzie, for always being there to listen to all the frustrations these projects created over the last 18 months.

I would like to express my greatest thanks to Dr. Denardo for the time and effort he has invested into my research projects and development as a student. I am one of his many thesis students in his long career. His dedication and contributions to educational physics has no doubt helped to develop scores of free thinkers and problem solvers. I enjoyed working on this project with him and tackling the many challenges we faced developing this experiment. His optimistic attitude kept me going through all of the seemingly impossible hurdles we encountered.

Furthermore, Dr. Godin is to be thanked for developing such an intriguing theory to research, as well as producing a theoretical model for us to compare our experimental data. He was very helpful in determining the regime under which we should collect data and what changes we needed to make with our apparatus to get there.

Lastly, I would like to thank NPS physics staff member Jay Adeff for all of the help he provided in this project. He was our go-to guy when we came across a problem we did not know how to solve. Jay also helped to track down hydrophones located in Physics Department's storage. He even spent a few hours working directly with me on the experiment at the height of the COVID-19 pandemic to get us closer to data collection, and attempted to use gating for data gathering.

THIS PAGE INTENTIONALLY LEFT BLANK

I. INTRODUCTION

A. BACKGROUND

As the global economy expands, the ambient level of acoustic noise in the ocean is increasing due to rising commercial shipping traffic, offshore drilling and piping for oil, as well as machinery used for harvesting hydrokinetic energy [1]. Curtains of air bubbles are used to suppress the high-frequency noise produced by these activities. Noise suppression in this scenario is mostly based upon a large volume of air contained in many small bubbles. The volume of air in the curtains creates an impedance mismatch with the surrounding water, and the bubbles also resonantly absorb sound [2]. In a theory article entitled "Passive, broadband suppression of radiation of low-frequency sound" by Godin and Baynes, [3] a different concept was introduced with a single volume of air being suspended in water to suppress low frequencies of noise in the water.

The use of a simple bladder or balloon to suppress acoustic emissions (for example, due to propellers) from Naval vessels offers a possible means of avoiding acoustic detection. Some progress has been made in this area by a research group in South Korea, using a membrane to suppress the noise created by cavitation produced by a propeller [4]. A controlled proof-of-concept experiment of the theoretical results of Godin and Baynes is required to justify continuation for further research in this area.

In this thesis, we describe an experiment in which a balloon of air is suspended underwater near a source of monofrequency sound in a low-frequency range. For each frequency, data were taken with and without the balloon being present and results were compared. Four main configurations of the apparatus were tested in the experiment (refer to Section B). This research project is the first attempt at a controlled experiment to compare to the theory, and the data show a promising trend. However, conclusive evidence was not found due to a myriad of experimental problems. COVID-19 played a part as well, forcing experimental research to halt for four months, slowing down all progress and limiting the available time for further controlled experimentation at a different location.

The tanks in the basement of Spanagel Hall offered a convenient location to conduct initial testing (Figure 1), but they were not sufficiently deep or wide, causing the received signal to be plagued with reflections off all of the surfaces of the water in the tank. The tank is lined with an anechoic material, but it only performs well at frequencies above 10 kHz. Due to parameter constraints (Section B), the maximum frequency in our experiment was 5.0 kHz. A larger facility is needed to defeat the reflections and obtain conclusive data through the use of signal gating.

For scale, the dimensions of the rectangular opening are 25 in. wide and 21 in. long.

Figure 1. Low-frequency noise suppression experimental apparatus

B. THEORY

The theoretical radiation pattern of a point source in water and near a spherical balloon is included in an article by Godin and Baynes [3]. The geometry is shown in Figure 2. The balloon has radius *a*, and the point source is a distance *b* from the center of the balloon, where $b > a$. The density of the fluid outside the sphere is ρ and the speed of sound is *c*.

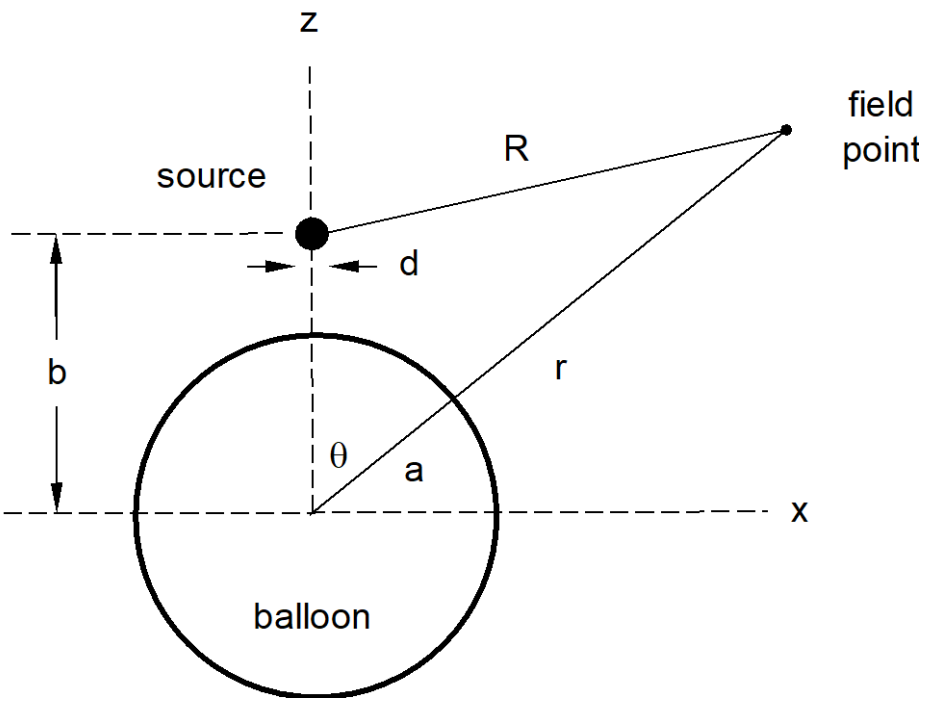

Figure 2. Geometry of an acoustic source near a spherical balloon, where $b >$ a. A point source (diameter $d \rightarrow 0$) is assumed in the theory.

According to the theory, the sound suppression is optimized for the following regime of parameters

$$d \ll b - a \ll a \ll \lambda, \tag{1}$$

where a, b, and d are the linear dimensions shown in Figure 2, and where the wavelength is $\lambda = c/f$, where c is the speed of sound and f is the frequency. We found that the condition (1), even if only roughly met, is difficult to achieve in an experiment.

To describe the acoustic wave due to the source itself, Godin and Baynes use $\boldsymbol{r}_0 = (0, 0, b)$ to denote its location. For convenience in our experiment, we let R be the distance from the source to the field point, as shown in Figure 2. In the experiment, we deal with $\theta = 0, 90^{o}, 180^{o}$, and 270^{o}, where the corresponding values of R are directly measured.

In the absence of a balloon, there is a spherical radiation pattern with pressure amplitude

$$P_{sph} = \frac{D}{R}. \tag{2}$$

where D is a constant having units of Pa·m. From Godin and Baynes, the amplitude of the total pressure in the presence of the balloon for $r > b$ is

$$P = kD\left|\sum_{n=0}^{\infty}(2n+1)P_n(\cos\theta)h_n(kr)\left[j_n(kb) - A_n h_n(kb)\right]\right|, \tag{3}$$

where $k = \omega/c = 2\pi f/c$, where f is the frequency and c is the speed of sound in water. In addition, P_n are Legendre polynomials, j_n are spherical Bessel functions of the first kind, and h_n are spherical Hankel functions of the first kind. For a "perfectly soft" sphere, which has a complete pressure-release boundary condition with negligible mass density of the fluid and negligible influence of the membrane, the quantity A_n in Equation (3) is

$$A_n^{(S)} = \frac{j_n(ka)}{h_n(ka)}. \tag{4}$$

For the more general case of a fluid-filled sphere of density ρ_F and sound speed c_F, the quantity A_n in Equation (3) is

$$A_n^{(F)} = \frac{Msj_n'(ka)j_n\left(\frac{ka}{s}\right) - j_n(ka)j_n'\left(\frac{ka}{s}\right)}{Msh_n'(ka)j_n\left(\frac{ka}{s}\right) - sh_n(ka)j_n'\left(\frac{ka}{s}\right)}, \tag{5}$$

where $M = \rho_F/\rho$ and $s = c_F/c$. The derivatives of the spherical functions are

$$g_n'(x) = \frac{n}{x}g_n(x) - g_{n+1}(x), \tag{6}$$

where g_n is j_n or h_n.

In our experiment, we measure the received voltage V with the balloon and V_{sph} without the balloon. These voltages are proportional to P and P_{sph}, respectively. We then graph the percentage difference of the two values as a function of frequency:

$$\frac{P - P_{sph}}{P_{sph}} \times 100\% = \left(\frac{P}{P_{sph}} - 1\right) \times 100\%. \tag{7}$$

To compare to theory, we require the ratio P/P_{sph}. From equations (2) and (3),

$$\frac{P}{P_{sph}} = kR\left|\sum_{n=0}^{\infty}(2n+1)P_n(\cos\theta)h_n(kr)\left[j_n(kb) - A_n h_n(kb)\right]\right|. \qquad (8)$$

For the case of an air-filled balloon in water, the quantity A_n in Equation (8) is approximately given by Equation (4), and more accurately by Equation (5).

II. EXPERIMENTS

A. APPARATUS

1. Overview

The basic design of the experimental apparatus is as follows: two hydrophones are placed at the same depth in an in-floor tank in Spanagel 025. One hydrophone acts as an acoustic driver, while the other acts as an acoustic receiver. Both hydrophones are displayed in Figure 3. According to the theory (Section I.B), we used a spherical balloon filled with air to act as a pressure release boundary. Also, according to the theory, the source should be small compared to the balloon, which is why we use a hydrophone as a driver. An extensive search for a sufficiently small underwater projector did not yield any such transducer. A transducer whose brand and model is unknown was found in the tank lab and was used in the experiment. For a significant reduction of acoustic radiation to occur, the balloon must be in close vicinity to the acoustic driver compared to the size of the balloon. Suspending the balloon was a major issue that required the creation of a special anchor (Section 3).

Left: Unknown cylindrical hydrophone used as an acoustic projector
Right: B&K 8103 hydrophone used as an acoustic receiver

Figure 3. Hydrophones to scale

2. Tow Tank

We used one of the two tanks in the tank lab in the basement of Spanagel Hall (Sp-025). These tanks have dimensions 21 feet long, 7 feet wide, and 7 feet deep [5]. One of the tanks was in use when experimentation began, so instead we used the "tow tank," outfitted with a tow mechanism. The tow mechanism does not interfere with the acoustics of the tank because it is completely out of the water. The tank's walls are lined with a rubber anechoic material that functions best at frequencies above 10 kHz

(Figure 4). The frequency range of the experiments were below that threshold, so the tank was not treated as anechoic, but there is expected to be some dampening of reflected energy off of the anechoic material compared to a concrete surface. The tank has a filtration system that can be run overnight to filter out some of the bacteria that grows in the tank.

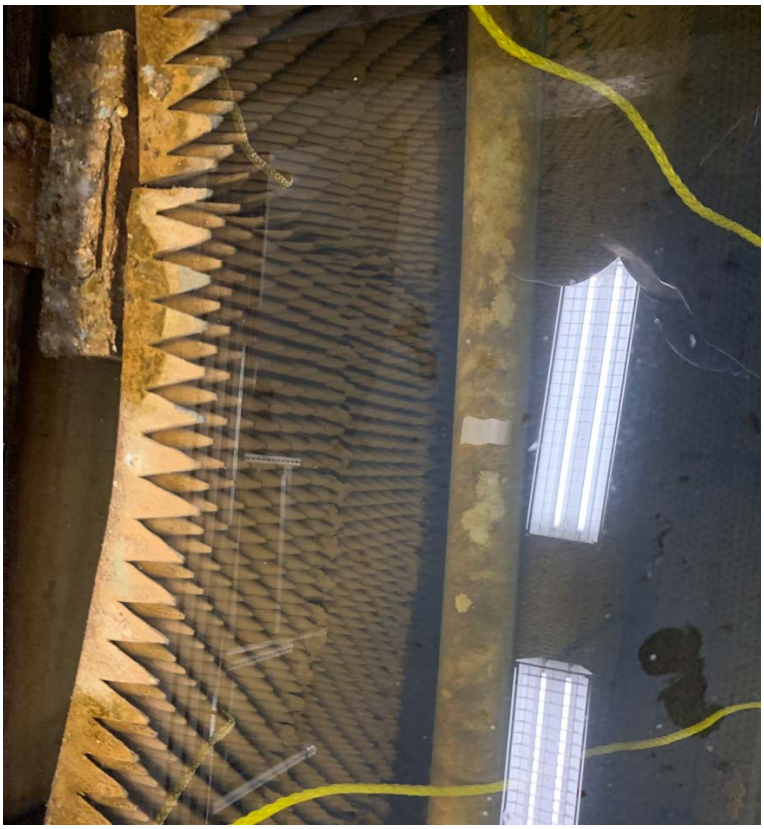

This anechoic material covers all surfaces of the tank and absorbs sound at frequencies greater than 10 kHz.

Figure 4. Anechoic material

3. Balloon Suspension Anchor

A balloon suspension anchor is needed to suspend a balloon underwater at a specific depth. The anchor needs to be sufficiently heavy to overcome the buoyant force on the balloon due the water. In addition, the weight of the anchor is reduced due to the buoyant force on it due to the materials used. The anchor was weighed down by two lead bricks shown in Figure 5. The anchor was constructed using two plastic plates bolted

together to hold two lead bricks; in air each brick weighs approximately 27.5 pounds and its dimensions are roughly 2 inches by 4 inches by 8 inches.

Figure 5. Lead brick

The dimensions of the plastic plates are 12 inches wide by 14 inches long and are 0.5 inches in height (Figure 6). They have milled recesses that are 0.375 inches deep so that the bricks could nest into the plastic to prevent the bricks from sliding out of the plastic plates. The plastic plates are bolted together using 6-inch long bolts that also acted as stilts, because the anchor would be sitting for long periods of time on the bottom of the tank which is lined with an acoustic absorber that mitigates reflections. Also attached to the plastic plates are eyebolts that are connected to cords that were used to safely raise and

lower the anchor, as well as adjust its position. In the middle of the top plate, a pulley was attached with a line that was used to adjust the depth of the balloon which was held by a plastic netting. A standard outdoor plastic netting is used to reduce the amount of deformation of the balloon as it is pulled against the buoyant force.

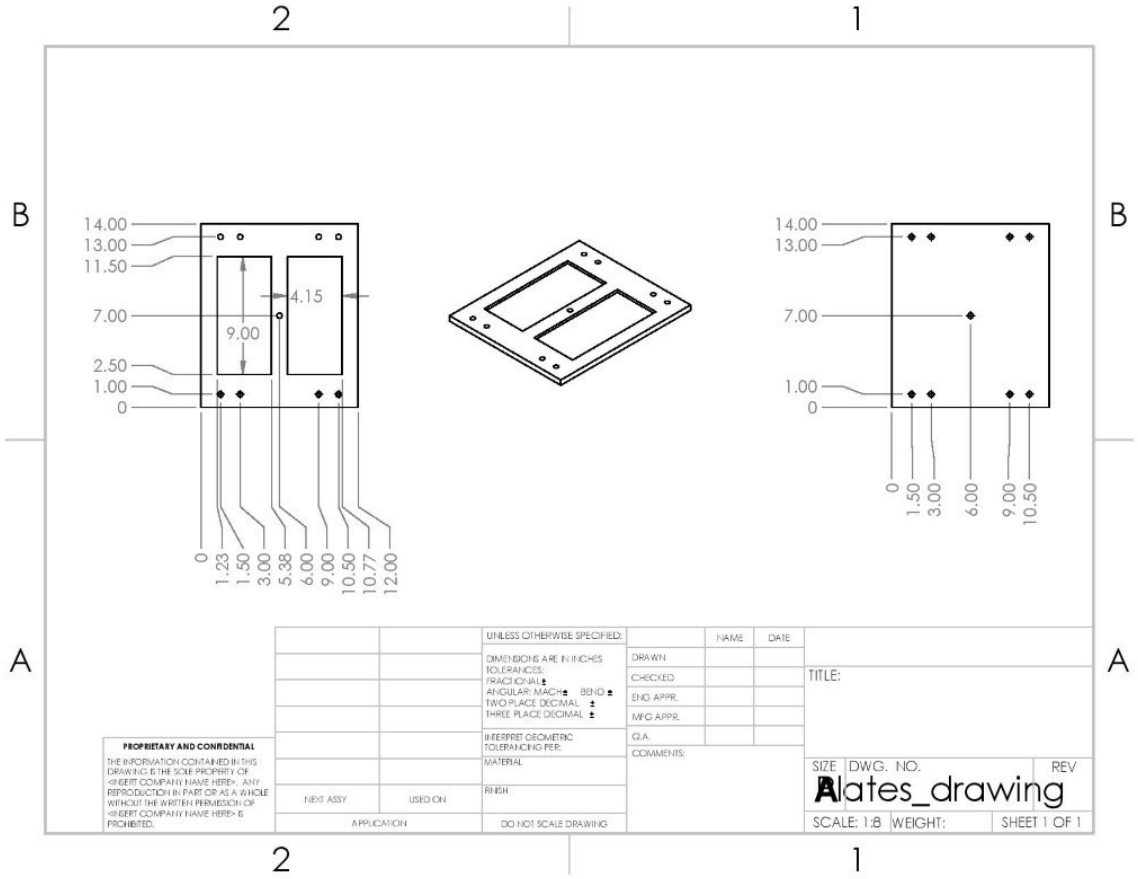

Figure 6. SolidWorks drawing of plastic plates used by an automated milling machine for the balloon suspension anchor

With the help of Physics Department model maker Mr. Steven Jacobs, we modeled the recesses and holes in the plastic plates using 3-D modeling software called SolidWorks [6]. A computer-controlled milling machine cut out the recesses and drilled through the plates for the stilts and eyebolts. Due to the deformities of the lead bricks, the original recesses were not sufficiently wide. We then used a manual milling machine to widen the recesses so that the lead bricks nested fully in the plastic plates. If a larger balloon is to be

used in the experiment, more weight will need to be added to the balloon suspension anchor, whose original design is depicted in figures 7 and 8. The suggested method to add weight to the balloon suspension anchor would be turning the lead bricks on their side so that two bricks could fit in each of the recesses, doubling the weight of the anchor. More manual milling may be required to fit both lead bricks in the recesses due to their deformities, but this can be quickly machined.

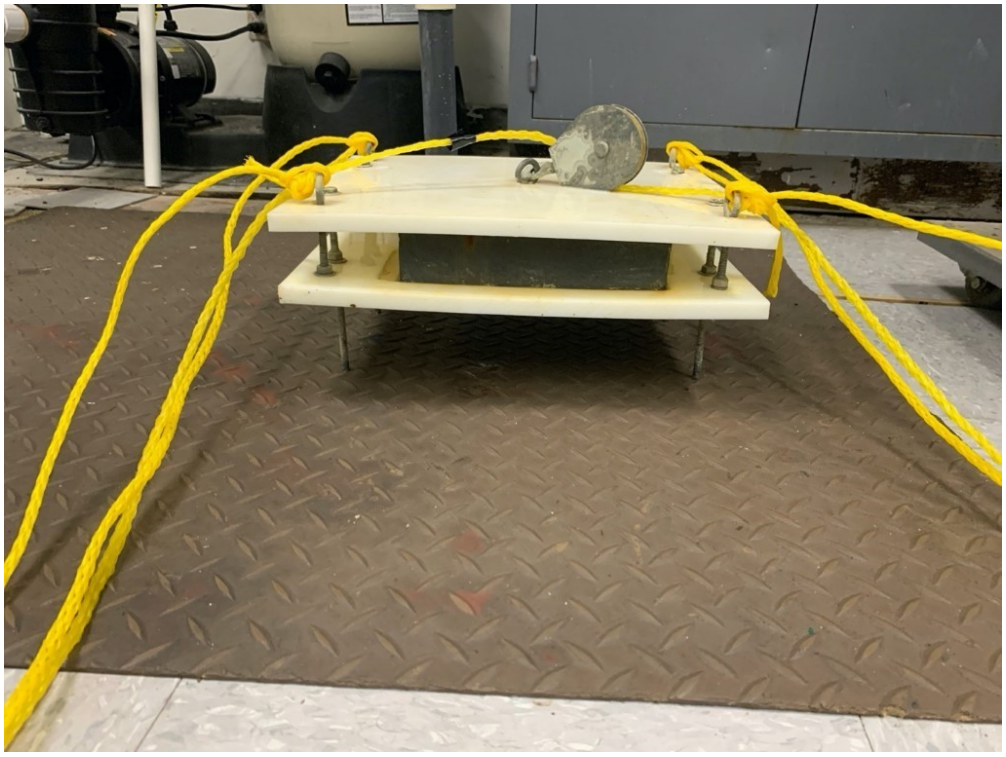

Lead bricks are sandwiched between plastic plates. A cord passing through the pulley is used to alter balloon depth. Cords around exterior are for adjusting the placement of anchor system. 6-inch bolts are used as stilts.

Figure 7. Side view of balloon suspension anchor

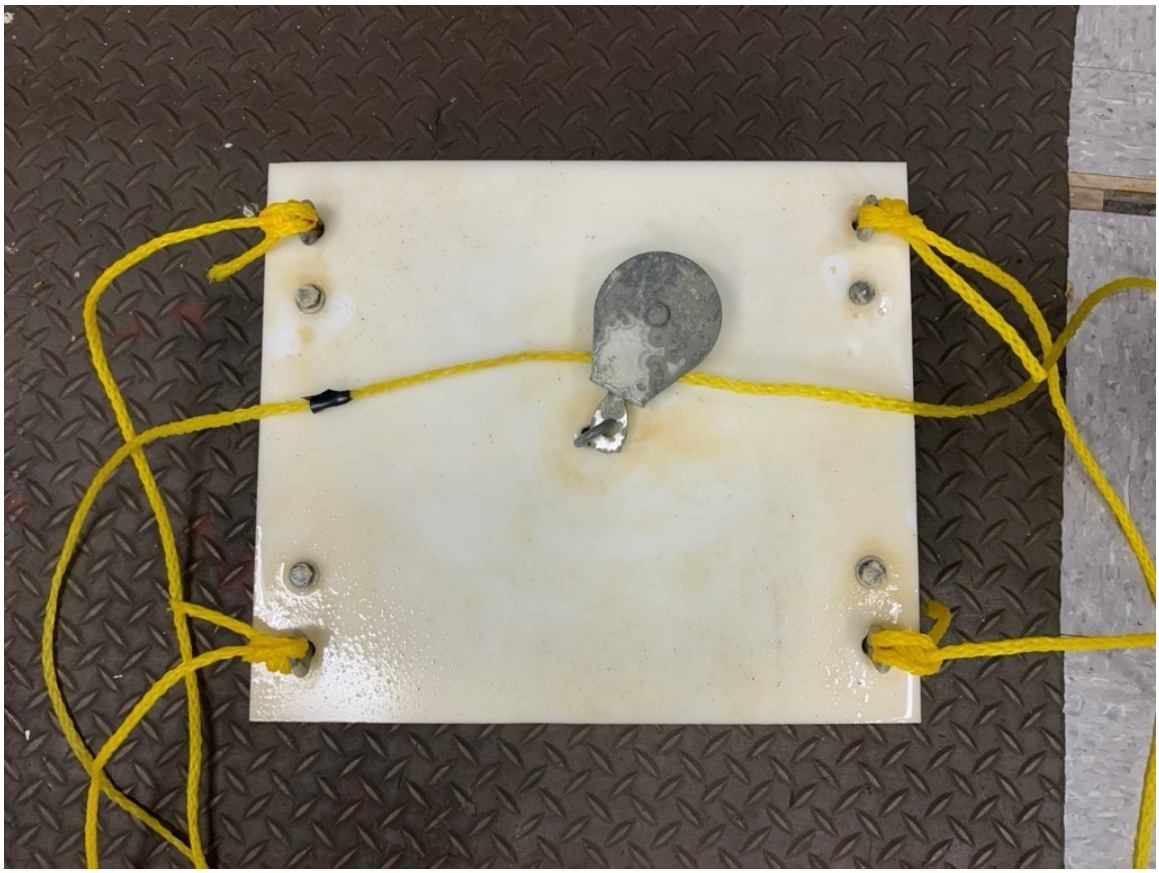

Lead bricks are sandwiched between plastic plates. A pulley is attached to the plates. A cord passing through the pulley in the center is used to alter balloon depth. Cords around exterior are for adjusting the placement of anchor system.

Figure 8. Top view of balloon suspension anchor

4. Underwater Lighting

Low-voltage pond lights were utilized in the tank. As Figure 4 shows, the water is not clear, even when the filters are run. An assumption is made that the use of chlorine could damage the anechoic material that lines the tank. To improve the apparatus further, lights were attached to an aluminum rod so that light could be seen in areas of the tank that were in shadows due to the location of overhead lights (Figure 9). Overhead lighting created large amounts of glare on the surface that made observing the location of the projecting hydrophone relative to the submerged balloon difficult. Submerged lighting eliminated this issue. Since they are low-voltage lights, they cannot under any circumstances be plugged directly into the wall. Since it is an electrical device being

submerged, this is a step taken to reduce the amount of current that could harm a human operator. To achieve low voltage, a Variac transformer was used, and was operated on roughly 8% to not blow out the bulb with too much input power. Three bulbs were lost troubleshooting this issue.

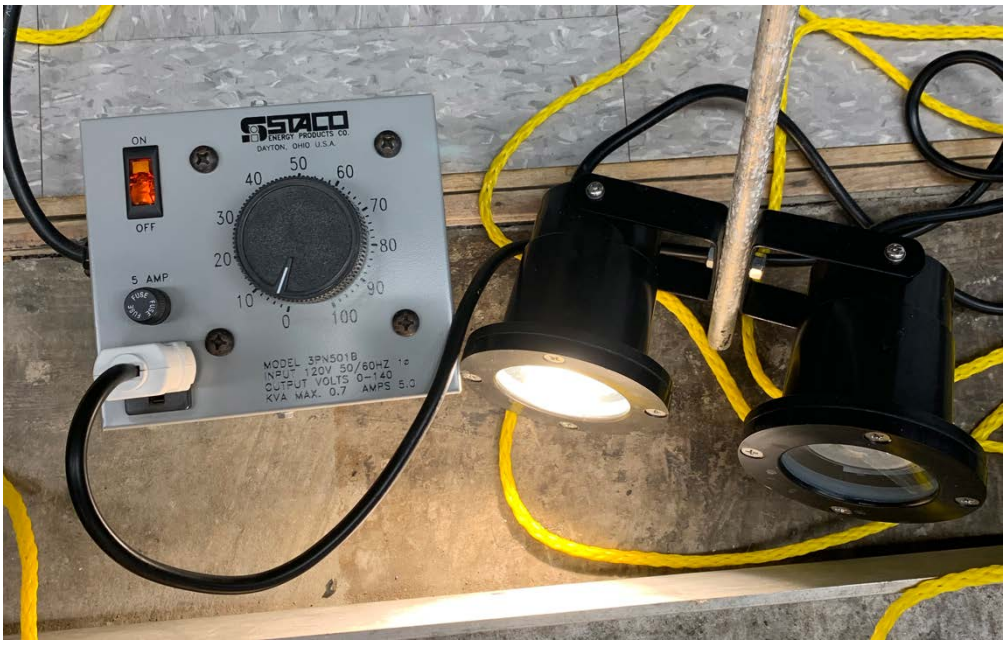

Figure 9. Lights and Variac transformer

5. Experimental Setup

The hydrophone chosen to be used as the receiver is a Bruel and Kjaer (B&K) 8103, and is expected to cost thousands of dollars. The projecting hydrophone used was an unidentifiable cylindrical hydrophone with a diameter of 0.375 inches and a height of 1.0 inch. It is also very delicate and expected to be quite expensive, as well. The hydrophones are displayed to scale in Figure 3 compared to a ruler.

A Techron 5530 power supply amplifier that produced a maximum peak drive voltage of 80V was used to drive the projecting hydrophone. A waveform generator was connected to the Techron power supply and was used to control the frequency, as well as fine-tune the voltage across the projecting hydrophone. The process was simple: turn the peak-to-peak voltage down on the waveform generator and turn the Techron power supply

amplifier to its maximum setting. Then adjust the peak-to-peak voltage on the waveform generator to show a 5V voltage across the projecting hydrophone on the multimeter.

Early testing found that there is a significant level of ambient noise that is detected in the tank from the other equipment running in the concrete building. Concrete slabs only weakly dampen acoustical energy. This running equipment could be anywhere in the building, so asking the entire building to shut off all of their machines was not reasonable. A Stanford Research Systems SR560 preamplifier was used to boost the signal and also filter out some of the noise in frequency ranges less than 300 Hz, so that it was easier to measure with a Stanford Research Systems SR850 lock-in amplifier. The lock-in amplifier was utilized to determine the amplitude of the received signal and improved the signal-to-noise ratio (SNR) substantially compared to the signal analyzer.

All of the equipment used to project and receive the signal was stored on a rack as shown in Figure 10. A balloon was attached to the balloon suspension anchor using cord and a plastic netting to reduce deformities of the balloon as the buoyancy force acts against the normal force keeping the balloon submerged shown in Figure 11. The receiving hydrophone was placed in its fixed position, and the projecting hydrophone was placed in its desired configuration. Tests were run in incremental frequencies using the waveform generator, and the balloon was added and removed for each frequency, and configuration. Five cleats were mounted to the tank grating to secure the balloon to a fixed depth when it was submerged and reduce the clutter of lines around the tank (Figure 12). A large amount of tension was created due to the buoyancy force, and the cleats reduced the amount of time between test runs due to simplifying the process. The other cleats were used to secure the balloon suspension anchor adjustment cords. A large knot was tied on the cord that was used to stop the cord from going too far through the pulley and ensuring that the balloon was submerged to the same depth every time it was lowered.

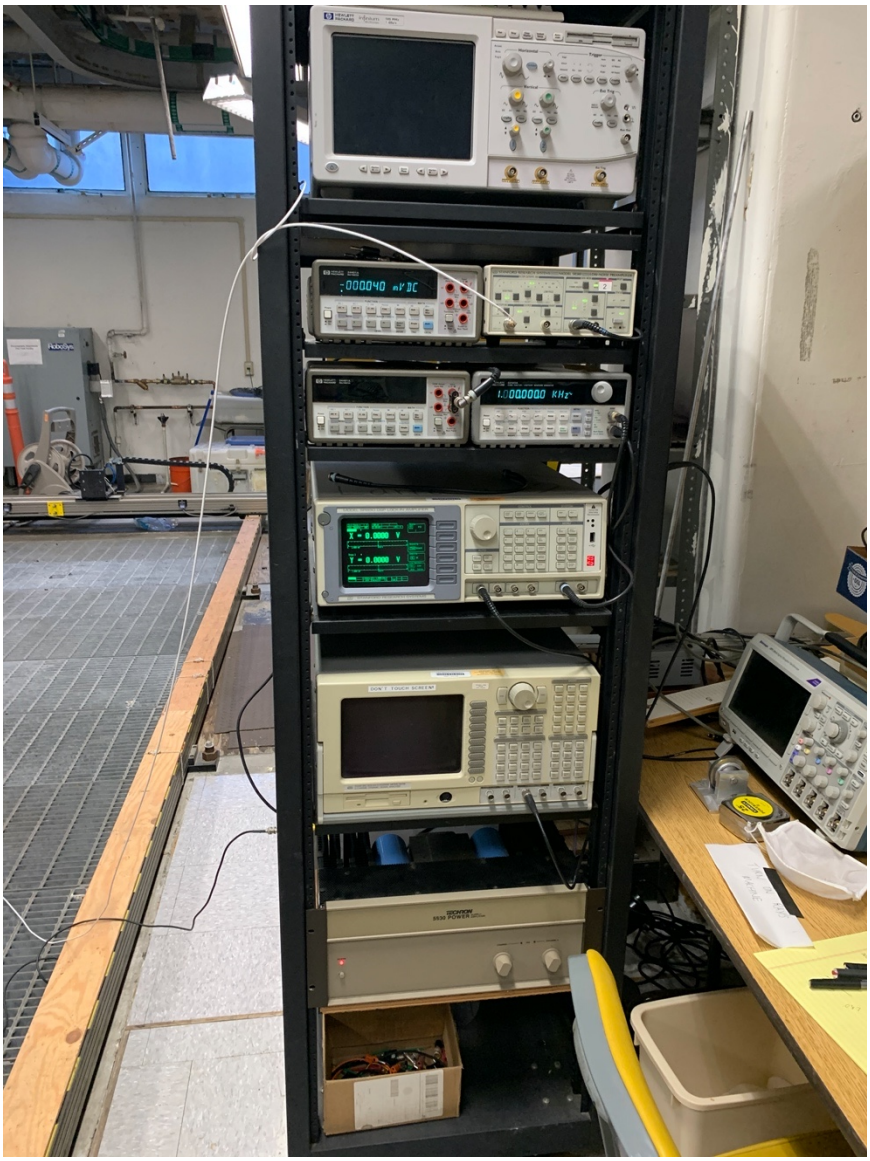

Figure 10. Equipment rack used in the experiment

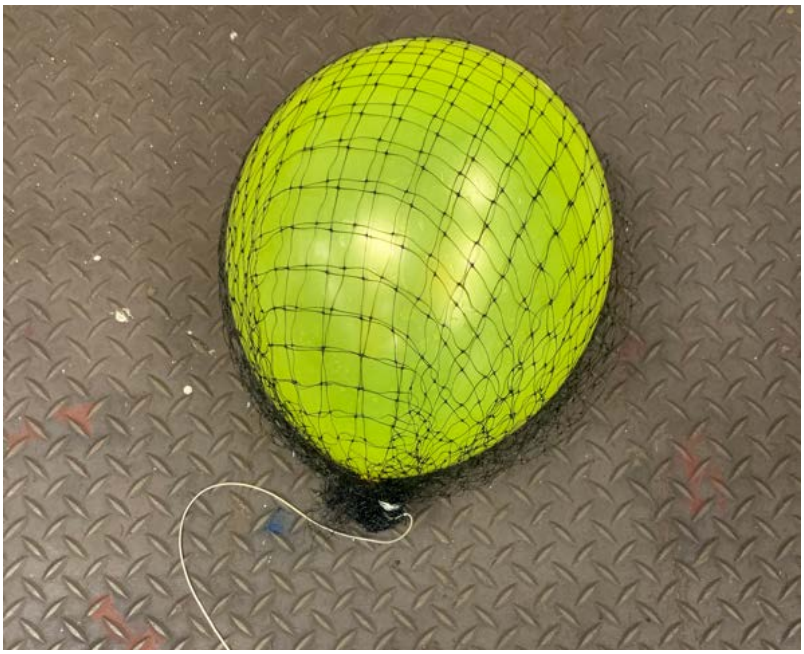

Figure 11. Balloon in netting

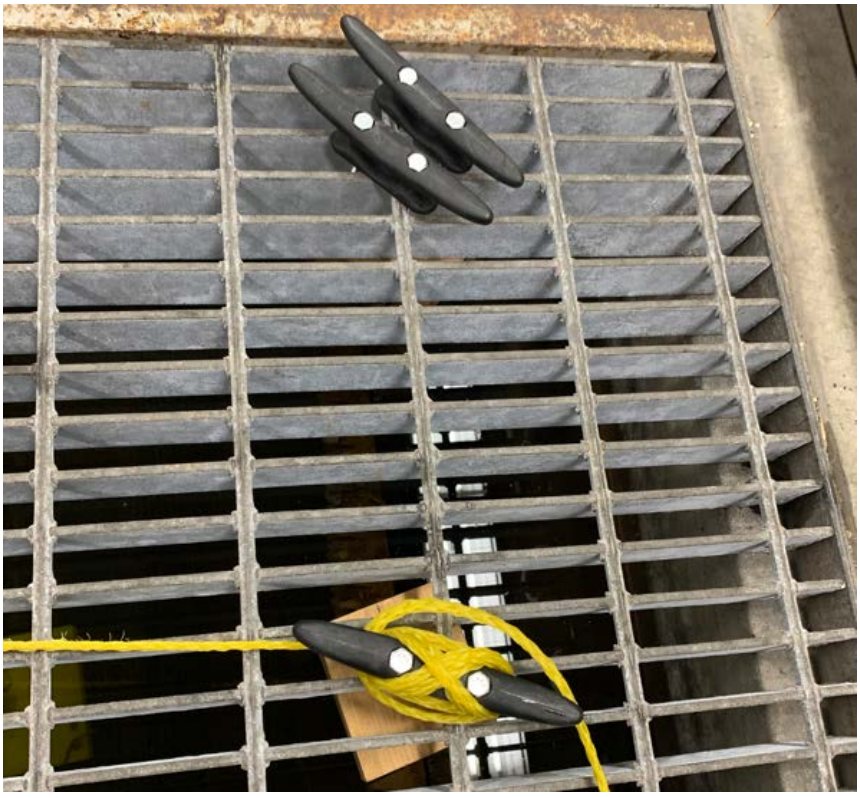

Figure 12. Cleats mounted to grating

B. INITIAL TESTING

1. Overview

Early experiments were run and slowly improved as we gained more experience with the equipment and changed the equipment. The behavior of the hydrophones appeared erratic at times. The oscilloscope was quickly abandoned due to the large amount of ambient noise in the building. Once a signal analyzer was used with averaging, fluctuations in most of the data points subsided. While it was very tedious to run through so many frequencies and so many configurations, data became more reproducible and cleaner with more practice and improvements to the experimental apparatus. Later, it was determined that reducing the drive voltage significantly and using a lock-in amplifier to remove the noise greatly reduced the occurrence of drifting and gave more trust to the experimental data.

2. Problems

On the very first day of testing, two hydrophones, the DT-574 and ITC-1032 were found that were high quality and are used for other acoustics experiments in courses that are offered at NPS. The initial setup used a smaller power amplifier to drive the hydrophones with a varying voltage amplitude. A multimeter was used to monitor the voltage driven across the hydrophone. A B&K 8103 miniature hydrophone was used as a receiver and was routed to a preamplifier which amplified the signal and was used in a high pass filter mode to remove noise outside of the selected frequency range. The signal then went from the preamplifier to an oscilloscope. Unfortunately, the power amplifier did not provide enough amplitude to the projecting hydrophone to attain a reasonable value due to the large amount of ambient noise present. Due to the small drive amplitude, a new power amplifier was used that produced much more amplitude, but there was still too much ambient noise present for a reading to be conducted. A transformer was located and borrowed from the physics lecture demonstrations laboratory and was put into the system. Now nearly 1000 volts were used to drive the ITC-1032 at 1 kHz, and a very large amplitude was present. The oscilloscope reading was unreliable at some frequencies. As the voltage across the hydrophone decreased, the received signal amplitude decreased to a

level where ambient noise was too high to obtain a trustworthy measurement. A Stanford Research Systems SR870 signal analyzer was used to extract the amplitude in the received signal at the drive frequency. This improvement gave us confidence for the first time that a reasonable data point could be attained from the setup. Unfortunately, as further testing was conducted, signal drift presented itself, and has been a problem in the experiment. Equipment was checked individually, and it was determined that the signal drift was not caused by faulty equipment. In the checking though, a capacitor in the power amplifier was found to be leaking, and was swapped with a new one. This new amplifier did not fix the signal drift problem though. Different projecting hydrophones were used, as well as different receiving hydrophones but these were not the source of the drifting signal.

Eventually, a set of data was taken that had minimal drifting present and was compared to a model using theoretical calculations. According to the theoretical model, it was found that the regime of our equipment would amplify the signal when the balloon is present instead of suppressing the signal. Some calculations were conducted, and it became clear that a much smaller diameter source was required. The ITC-1032 hydrophone had a 2.5-inch diameter and it was switched out with a hydrophone that has a 0.375-inch diameter. The receiver was moved closer to combat the reflections that were present in the tank in an attempt for gating to be used.

Reproducibility became a major issue when the experiment was first run. When driving the new hydrophone at 100V using the transformer, drifting was a very bad problem at many data points, so much so that a full set of data was not able to be taken at any configuration. A hypothesis for the source of the drifting was that the projecting hydrophone was being overdriven, so the transformer was removed, and the hydrophone was only driven by the power amplifier. A new set of data was taken at a drive voltage of 50V. Drifting was much less visible in this data set, but there were a few outliers that did not correspond to the trends that were present among the rest of the data set. Another set of data was taken at a 20V drive voltage, and there were fewer outliers, and the same general trends were observed. The data was much less volatile, but drifting was still present, and not as often. In hopes to remove the drifting completely, another data set was taken with a 5V drive voltage, and this was the cleanest and least volatile of the three sets

of data. A lock-in amplifier was required due to the very low amplitude signal received by the B&K receiving hydrophone. The set of data taken with a drive voltage of 5V was the final data used in the results of this experiment.

Another hypothesis that would not describe the drifting but could possibly describe the difference in received amplitude was that reflections present in the signal were strongly dependent upon the exact location of the source and receiver. A test on this sensitivity was conducted and the results are shown in Figure 13. The projecting hydrophone was moved an inch in all directions, one axis at a time. The percent difference in each direction on each axis were averaged and are displayed on the bar graph. As can be seen from the amounts of error in each of the axes at each configuration, none of them account for 400% deviations in received signal. Both sides were not measured because they are expected to behave symmetrically.

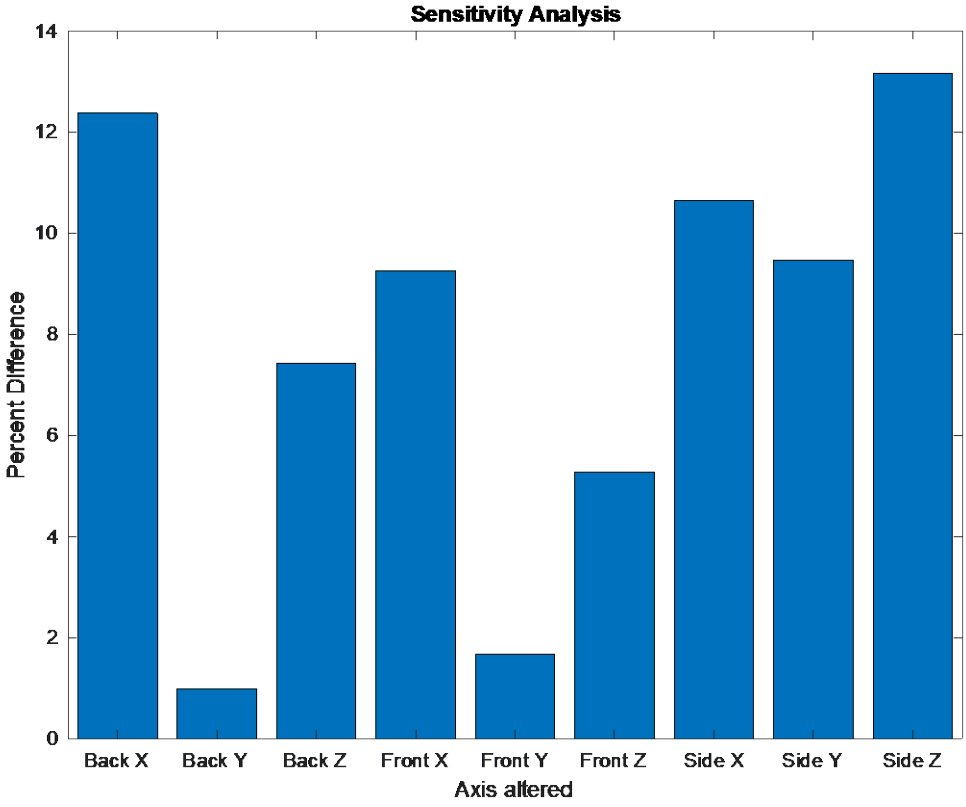

Figure 13. Sensitivity analysis of hydrophone displacement

3. Apparatus Improvements

Changes were made to the experimental apparatus such as securing the receiving hydrophone to the tank so that its position could be more exactly recorded and reproduced (Fig. 14). It was secured using square tubing to create an even surface across the grating, and weights were placed on the square tubing to hold them in place. A 90-degree clamp was used to secure the receiving hydrophone to the vertical rod.

Figure 14. Receiving hydrophone structure

There was also a need for securing the projecting hydrophone to the tank due to the uneven surfaces the tank grating created. It was just slightly taller than the tank grating access frame. The ridges on the grating caused the tubing to sit on an uneven surface. The first attempt to fix this problem was to switch out the round aluminum tubing for square aluminum tubing. Unfortunately, the grating became more of an issue due to the increased

width of the tubing. Two square lengths of tubing were cut to match the width of the tank grating access frame and were secured using C-clamps to the frame, shown in Figure 15. The lengths of square tubing to create a raised flat surface were arranged parallel to each other.

Figure 15. Rails for projecting hydrophone structure

The square rod attached to the aluminum rod that held the projecting hydrophone was also secured to the parallel lengths of square tubing using more C-clamps (Figure 16). The rod that was attached to the projecting hydrophone and allowed for vertical adjustment was secured to the square rod using another 90-degree clamp.

Figure 16. Projecting hydrophone structure

Later it was found that the aluminum rod that was attached to the hydrophone using plastic zip ties was reacting to the water in an expected hydrolysis reaction. It is very common for aluminum to react in this manner and produce a hydrogen gas. Hydrogen bubbles were formed along the rod due to the expected hydrolysis reaction, and to reduce the error in terms of experimental reproducibility, both aluminum rods were switched out for stainless-steel tubes.

As the balloon was submerged, it was subjected to major deformation as a greater downward force to pull the balloon down to a preset depth was put on the balloon. The balloon flattened out and would break if it was pulled down too quickly. A thin plastic netting was used to more evenly distribute the downward force throughout the whole balloon. This resulted in a much more spherical shape which corresponded more closely to the theory. The rope used to suspend the balloon was tied through the netting as well, to

put as little load on the balloon as possible, in hopes to elongate its life in the experiment. It was a time-consuming task to switch out balloons so the longer it lasted, the easier it was to collect data and troubleshoot the major issues that occurred.

4. Selection of a Hydrophone as a Source

The experiment requires a low frequency source (roughly 500 Hz to 5.0 kHz), which proved to be very difficult to find. Since the size of the source must be significantly smaller than the balloon, a smaller source is better because the buoyancy force of the submerged balloon greatly increases with an increasing balloon diameter. After searching the Physics Department's storage for unused hydrophones, a few different possible sources were tested to assess their applicability for this experiment as both a source as well as a receiver. The tests were all run at the maximum drive voltage that the hydrophone could handle before distortion was present. The waveform generator was set at 1.0 kHz, the preamplifier had a gain of 100, and the bandpass filter was set from 100 Hz to 10 kHz. The hydrophones were switched out one after the other keeping everything else constant. The received amplitude was read from the signal analyzer, and the noise was observed using the oscilloscope. Later, we found that some of the noise was due to having the transformer in close proximity to the waveform generator. Most likely some sort of magnetic field interaction was taking place which was affecting our results.

The results of our search for a source are shown in Table 1. In view of the theory for a point source, we selected the spherical transducer ITC-1032 for use as a driver. Later it was determined that the smallest source that gave the strongest signal was needed due to the relatively large 2.5-inch diameter source. In this testing, to overcome the high ambient noise level, we used a transformer (Pasco SF-8616 Basic Coil and Core Set) which was able to step up the voltage roughly 8:1 from a 5530 Techron Amplifier. The amplifier produces a maximum drive voltage of 80 Vrms, while we were able to drive the ITC-1032 source using the transducer to roughly 1000 V. Without the transformer, the hydrophone was not easily heard by the human ear, and the received amplitude was in the low microvolts range even with a large gain from the preamplifier.

For the smaller hydrophone used reversibly as a source, the transformer was not needed because the hydrophone could not handle high voltages. This is the reasoning that the result of this testing for the unknown cylindrical source resulted in a large distortion. To overcome the SNR, a much higher gain on a preamplifier was implemented, and a lock-in amplifier was used. Additionally, to improve the reproducibility, the drive voltage was reduced drastically from 300V using the ITC-1032 hydrophone with a transformer, to 5V using the smaller unknown hydrophone. About 30 seconds of operation was needed to determine the received signal at all recorded frequencies using the lock-in amplifier.

Table 1. Hydrophone analysis

Hydrophone	Diameter	Received Amplitude (mV RMS)	Results
DT-574	4″	15.00	Good noise ratio, noise is not dominating signal.
ITC-1032	2.7″	14.97	Good noise ratio, noise is not dominating signal
ITC-1089	1/2″	1.50	40V Techron source limitation, not much amplitude
Unknown Cylindrical	3/4″	2.65	Overdriving it, bad distortion, low amplitude
Unknown Spherical	1″	3.00	Overdriving it, not much amplitude, bad distortion

Comprehensive analysis of the possible hydrophones used as sources and their behavior at a standard drive frequency and voltage.

When running similar trials to choose the best receiver, the B&K 8103 was chosen. When looking at the signal from a driven transducer on the oscilloscope, it was very clear that the B&K 8103 was the best receiver due to the sensitivity as well as the lack of transients that were present when the DT-574 or the ITC-1032 were used as receivers.

C. PROCEDURE FOR GATHERING DATA

About an hour before data gathering, it may be worthwhile to turn on all equipment and let it "warm up." More testing is needed to see if this helps reduce reproducibility error in the experiment. The lock-in amplifier, power supply amplifier, preamplifier, and the multimeter that measures the voltage across the projecting hydrophone are required to be turned on prior to use.

The steps listed below were followed for data collection.

1. Position receiving hydrophone at standard location.
2. Put balloon in tank. Position source at desired location near balloon. With power amplifier knob turned to maximum, adjust the amplitude on the waveform generator to get to 5.0 Vrms on the multimeter.
3. Take hydrophone readings for 0.5 to 5.0 kHz in increments of 0.5 kHz. Turn power amplifier gain knob to zero *each* time before changing frequency.
4. Remove balloon from tank, and repeat measurements in step 2.
5. Repeat steps 1–4 until all eight sets of data are acquired.

III. DATA ANALYSIS

A. OVERVIEW

The configurations used in the experiments are displayed in Figure 17.

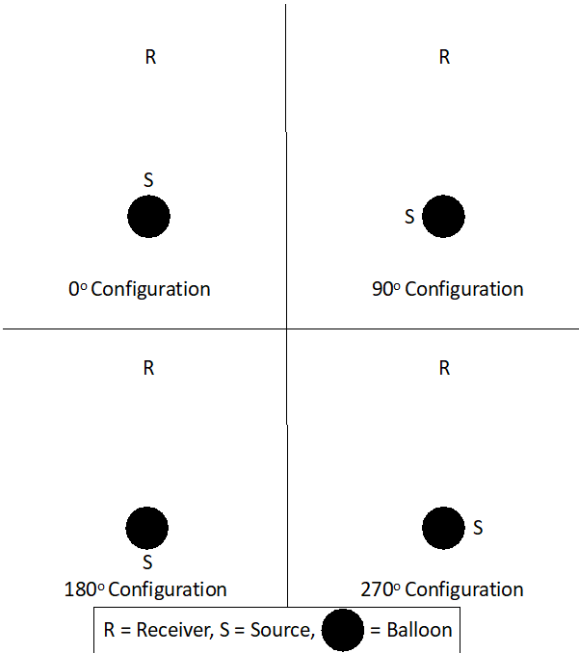

Figure 17. Steady-state hydrophone configurations

Listed in Table 2 are the chosen parameters based on the theory to create a regime where the presence of the balloon reduces the received amplitude of the signal. The geometrical parameter notation follows Figure 2. The radius of the balloon is *a*. The distance from the center of the balloon to the center of the projecting hydrophone is *b*. The distance from the center of the balloon to the center of the receiving hydrophone is *r*. Parameters *a*, *b*, and *r* do not change because the only quantity changing in each configuration is the position of the projecting hydrophone. The projecting hydrophone is placed the same distance from the edge of the balloon each time. Parameter *R* is the distance from the center of the projecting hydrophone to the center of the receiving hydrophone, which is the only changing parameter. Parameters *M* and *s* are also constant for all configurations because they are based upon the environment of the tank which is not changing for any configurations. *M* is the ratio of density of the fluid inside the balloon to

the density of the water in the tank, and *s* is the ratio of the speed of sound of the fluid inside the balloon to the speed of sound in water. An important note is that the 90-degree configuration and the 270-degree configuration are mathematically equivalent, and their results are anticipated to be symmetrical with some experimental error.

Table 2. Parameters of configurations

configuration angle θ	**a (m)**	**b (m)**	**r (m)**	**R (m)**	**M**	**s**
0º	0.1217	0.1519	2.540	2.388	0.001225	0.237
90º	0.1217	0.1519	2.540	2.545	0.001225	0.237
180º	0.1217	0.1519	2.540	2.692	0.001225	0.237
270º	0.1217	0.1519	2.540	2.545	0.001225	0.237

B. REPRODUCIBILITY

This experiment had a serious reproducibility issue, as described in Section II.B.2. The trends are mostly followed in the 0-degree configuration (Figure 18), although there were problems even with the lowest voltage cases. All of these tests were conducted on different days, and the same startup procedures were followed. For low frequencies of 2.0 kHz and below, there is minimal, even negligible difference between the responses at different drive voltages. Major discrepancies begin at 2.5 kHz, and in multiple trials large oscillatory differences begin to deviate from each other. The most prevalent reasoning for these differences would be that this is a hydrophone meant for receiving signals, and its performance as a driver may not be consistent. The piezoelectric design allows for it to be used reversibly as a driver, but it is possible that the hydrophone was optimized to be used as a receiver which could limit its effectiveness as a source of sound. The B&K receiver used in the experiment has a very strong reputation and is very sensitive. It is clear though, that using a lower drive voltage is optimal in this experiment not only due to the absence of drifting present in the testing, but also to reduce fluctuations in the ratio calculations.

While there were substantial fluctuations in all of the data sets, reproducibility was confirmed as more data was gathered.

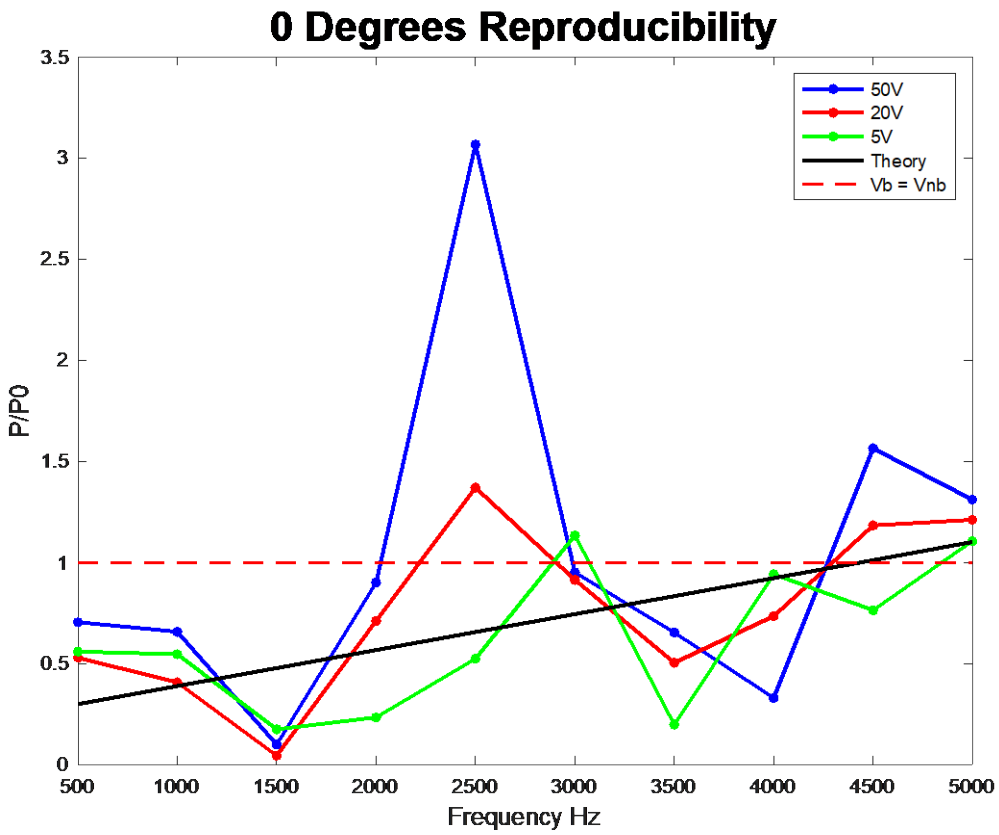

Figure 18. 0-Degrees reproducibility plot

Three more configurations were tested on different days at different drive voltages and are displayed in Figures 19 through 21. These figures confirm the reproducibility and for now, the extreme deviations are ascribed to poor source performance, and all possible systemic issues with the experiment have been examined and ruled out.

In some cases, even at a 5V drive amplitude, there are points that are more volatile than at the higher drive amplitudes, such as the data point at 5.0 kHz in the 90-degrees configuration in Figure 19. This large deviation is expected to be attributed to poor hydrophone performance as a driver, not a systematic problem since it behaves erratically. There are spikes that occur at different frequencies in the 90-degrees and 270-degrees configurations that this is also attributed to. The difference in the location of the spikes is expected to be related to the same drifting phenomenon that we observed at higher drive voltages. In contrast, at 180-degrees displayed in Figure 20, it is clear that a 5V drive amplitude gives the cleanest regime, as well as the least volatile, with a peak at 2.5 kHz with a magnitude roughly 50% less the other drive voltages.

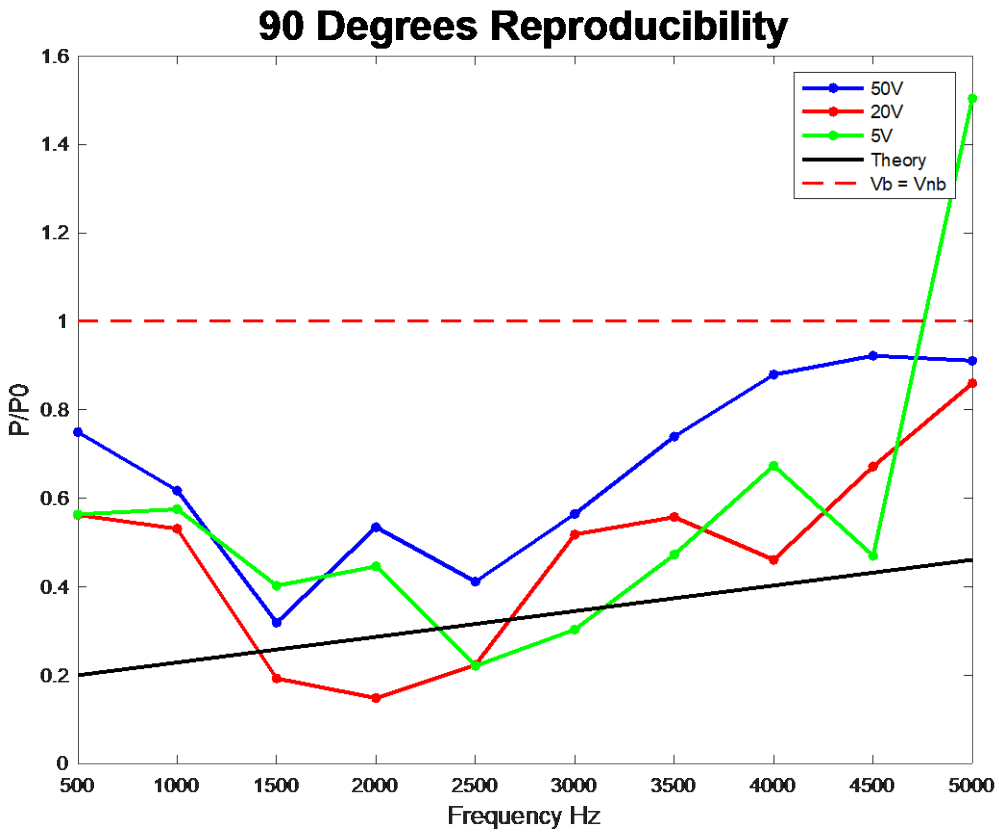

Figure 19. 90-Degrees reproducibility plot

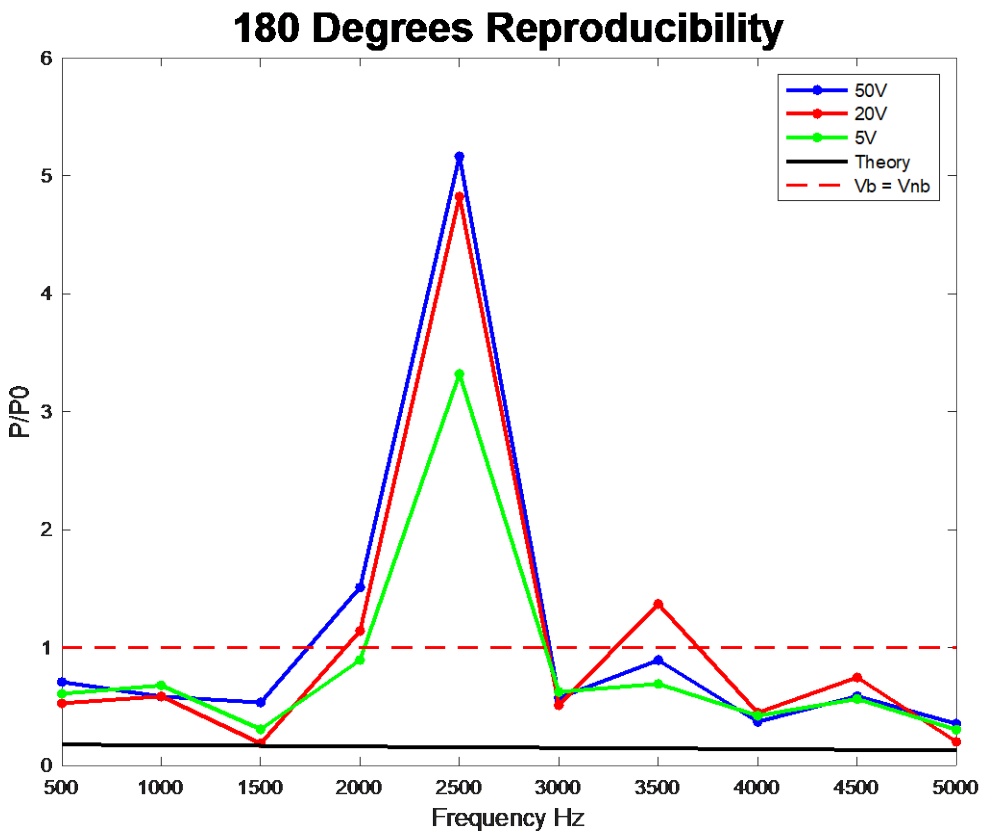

Figure 20. 180-Degrees reproducibility plot

Reflections are also contributing an unknown amount of error to the received amplitude, but these should still be reproducible and will not become a factor until conclusive data is to be recorded in a larger tank. In some of the configurations a 5V drive amplitude was recorded on two separate occasions for more overlap to prove reproducibility.

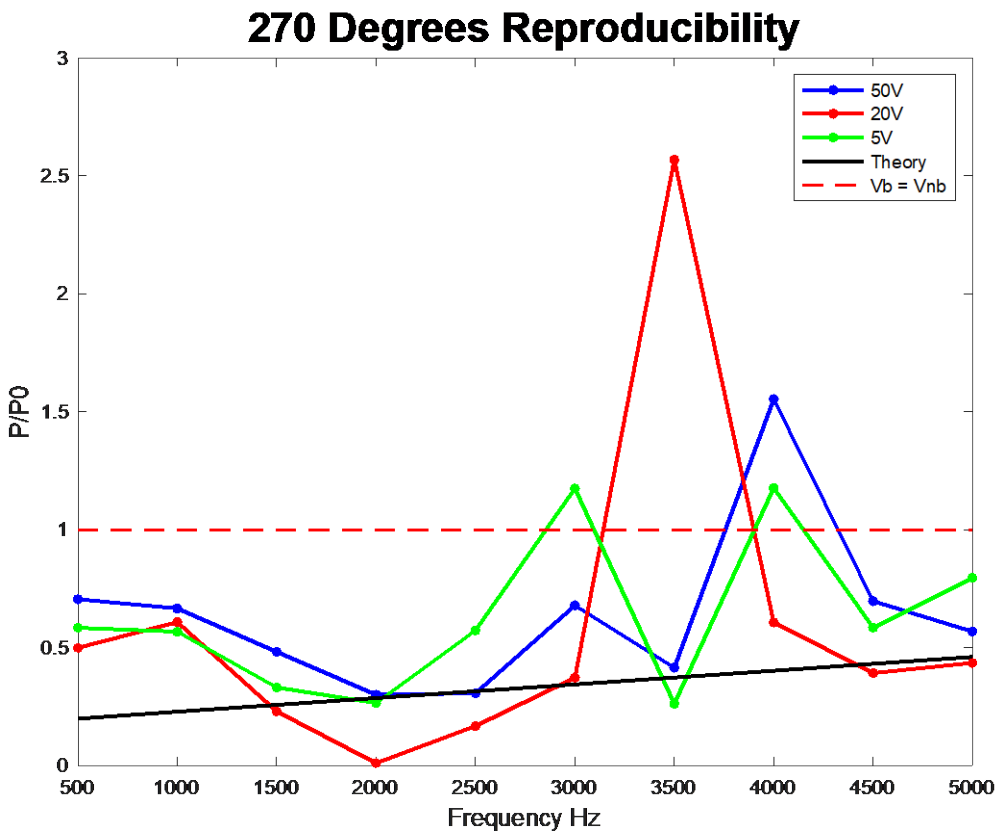

Figure 21. 270-Degrees reproducibility plot

C. COMPARISON TO THEORY

Figure 22 shows an overlay of the soft sphere (perfect pressure release boundary condition) theoretical curve onto the experimental data for the 0-degrees configuration. Theoretical curves for our geometrical parameters for non-zero values of *M* and *s* (Section I.B) for air are included in the Appendix, for all configurations. The experimental results were extremely promising in all configurations, even though reflections were present. The experimental data followed the theoretical value fairly closely in all four configurations. The differences are hypothesized to be related to the reflections that are present in the signal, as well as possible inaccuracy due to using a piezoelectric hydrophone as an underwater projector. In a larger tank, reflections would be present, but their signal would be able to be removed using gating. For the 0-degrees configuration shown in Figure 22, the theory line went through the middle of the data set, which was accurate even without

the ability to remove reflections from the received signal. The experimental data is plotted in blue, with the theoretical simulation plotted in a black line. The red dashed line shows where the presence of the balloon had a greater received amplitude than the "no balloon" trial.

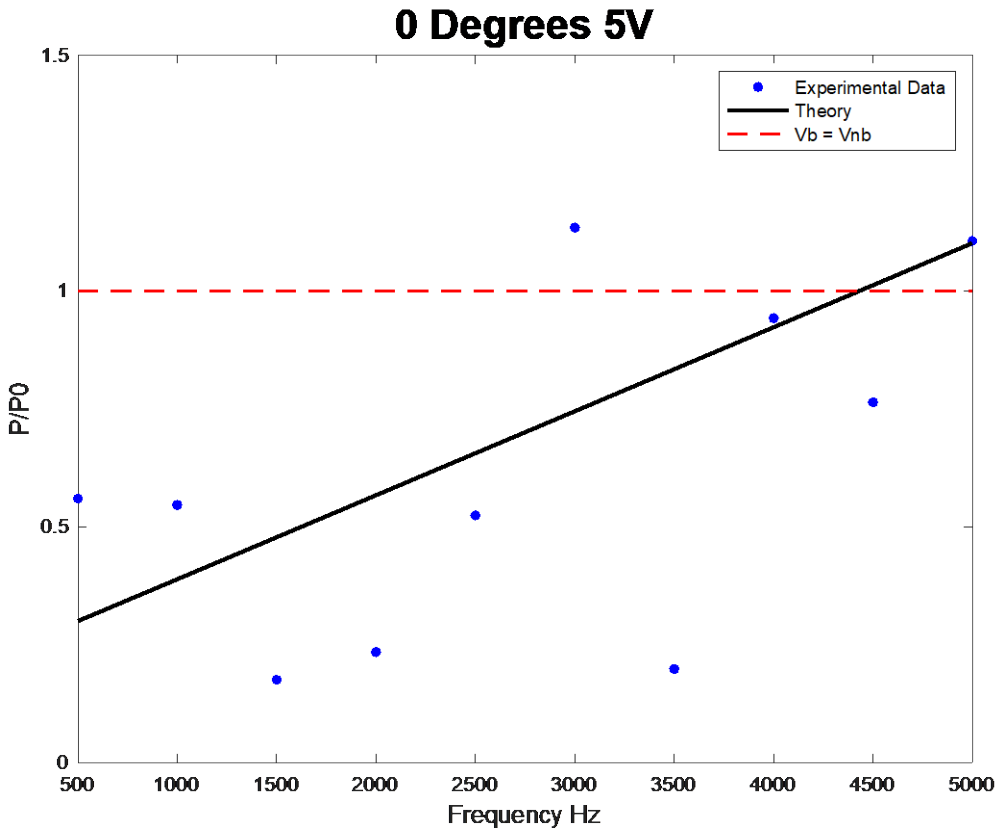

Figure 22. 0-Degrees configuration experimental data

For the 90-degrees data displayed in Figure 23, the theory line was below the experimental data. This is attributed to the increased effect of reflections due to the source being closer to one side of the tank than it was in the 0-degrees configuration. While the theoretical ratios were less than the experimental values, the slope of the experimental data is similar, and one could reasonably hypothesize that removing the reflections would make this data set more closely mirror the theory line. There is one data point at 5.0 kHz that must be noted when analyzing this graph. It is roughly a 150% greater ratio the other ratios.

An argument could be made to normalize it with the general trend of the other data points using a curve fitting model, but it was left to show that there were occasionally data points that could not be explained. The hydrophone being driven as a projector is expected to be the source of error because this extreme deviation was not observed when using larger drive voltages. More testing must be conducted to confirm this reasoning for the outlier in the data in this configuration.

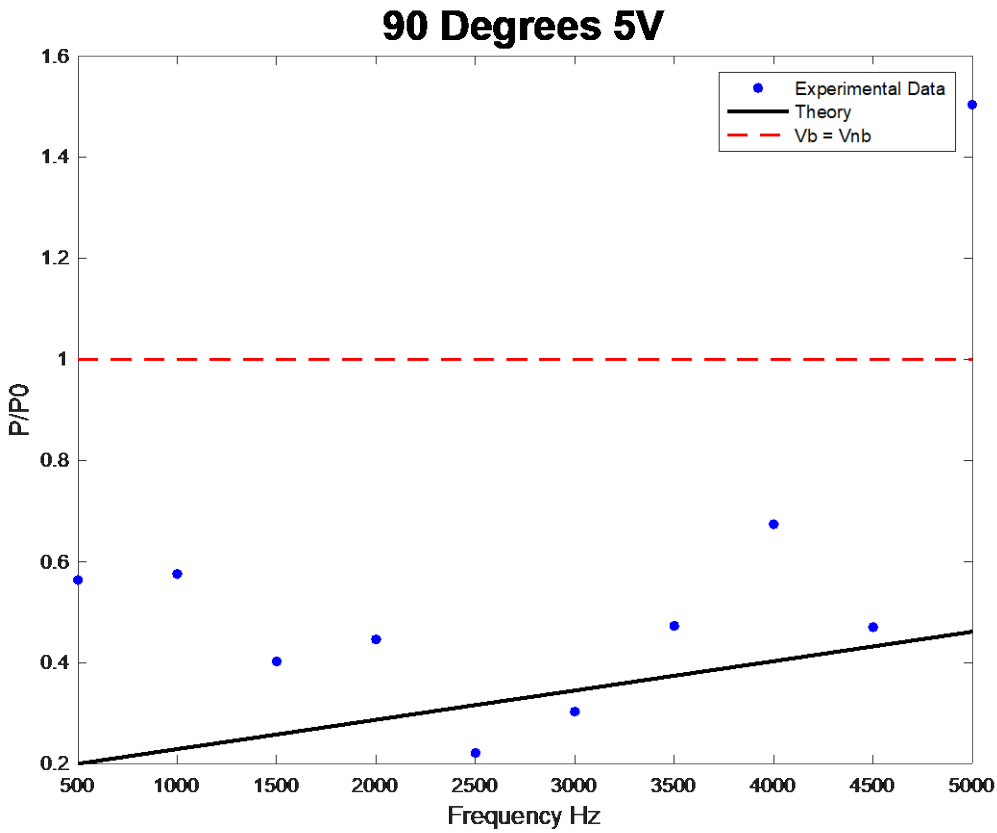

Figure 23. 90-Degrees configuration data

In the 180-degree experimental configuration shown in Figure 24, the experimental data were also a greater magnitude than the theory ratio values at all points. In this configuration, there will be fewer direct path rays to the receiver, so it is not unreasonable to say that the reflections off of the edges of the tank had the most effect in this configuration than in the other configurations. Interestingly, this configuration has an

overall decreasing trend with increasing frequency, with yet another major outlier shown at 2.5 kHz. This outlier in the 180-degree configuration was confirmed by testing at different drive voltages, described in Figure 20. This outlier is either strong reflections that hit a maximum amplitude based on the wavelength and the exact distance between the source and the receiver, or there is some kind of resonance with the balloon. At other configurations, 2.5 kHz does not show a substantially higher received signal, so this is not anticipated to be the reason behind this peak, but it should be investigated further.

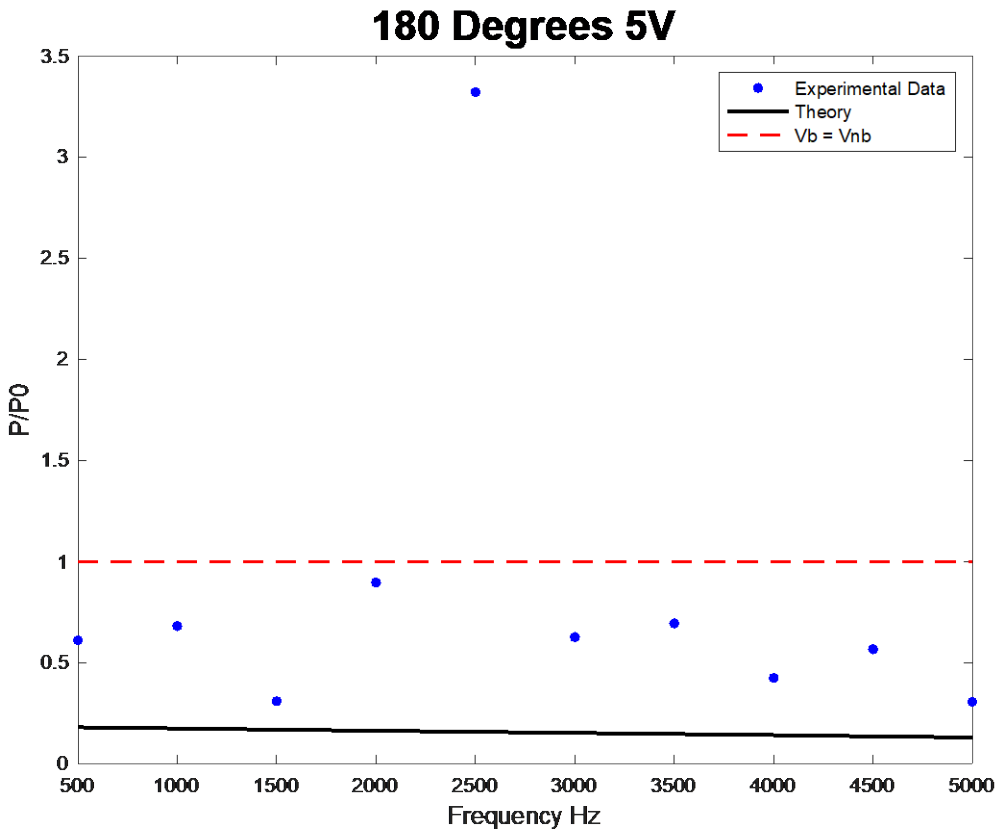

Figure 24. 180-Degrees configuration experimental data

In the 270-degree configuration in Figure 25, the theory is slightly less than the experimental data, but this can again be easily hypothesized to be related to reflections that are present in the tank. The slope of the theoretical approximation appears to follow the experimental data very reasonably.

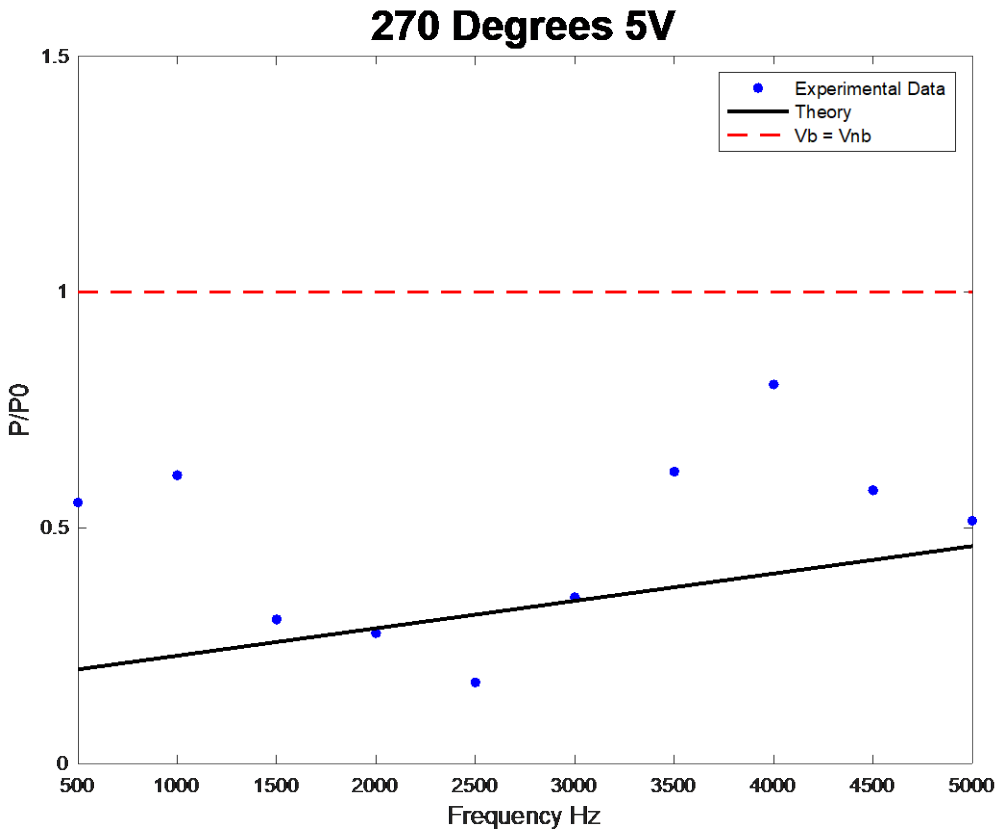

Figure 25. 270-Degrees configuration experimental data

Ideally, the 90-degree and 270-degree configurations should be equivalent, so the experimental data should be very similar. Figure 26 confirms this, aside from the outlier in the 90-degree configuration at 5.0 kHz.

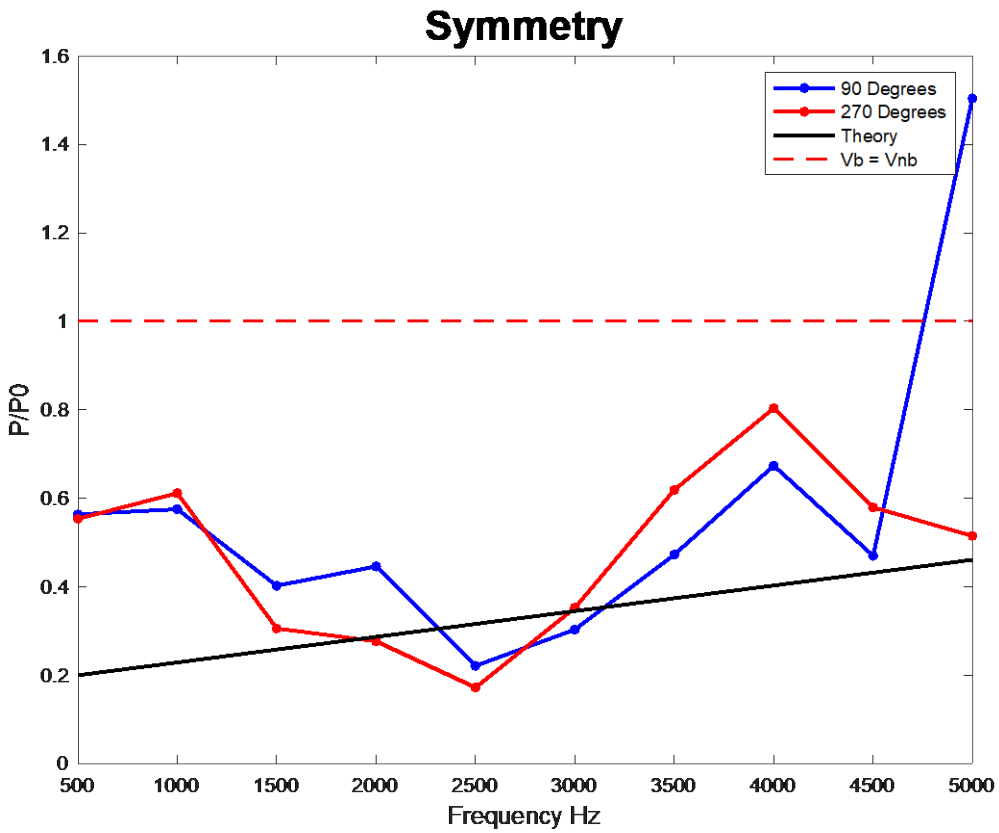

Figure 26. Symmetry of 90-degree and 270-degree configurations

Future testing removing the reflections from the received signal should prove to be extremely exciting!

THIS PAGE INTENTIONALLY LEFT BLANK

IV. CONCLUSIONS AND FUTURE WORK

A. SUMMARY

For a range of parameters, a balloon filled with air near a low-frequency underwater acoustic source is predicted to cause a significant reduction in the amplitude of sound. We have performed a first controlled experiment of this effect. The collected data displayed a very promising result when plotted with the theoretical curve. The agreement between the theory and the experimental data was only very rough, however, and the deviations are believed to be caused by reflections off the air surface and the walls and bottom of the tank. Due to campus restrictions associated with COVID-19, testing was halted for several months, and further testing was not possible due to time constraints. Testing will continue on this experiment with a follow-on student and will be conducted in a larger tank, most likely the NPS SLAMR facility (Section C).

B. GATING ASSESSMENT

The tanks in the "tank lab" in the basement of Spanagel Hall offered an extremely convenient location for initial research testing. Due to our minimal experience in underwater acoustics experiments, there was a steep learning curve with understanding the equipment and the environment. As more experience was gained, it quickly became obvious that there were major limitations that the tank created that were going to be unavoidable in the future. There is a very expensive anechoic lining in the tank that is only anechoic at frequencies greater than 10 kHz. For the parameter regime of this experiment, the frequencies ranged from 0.5 kHz to 5.0 kHz. It was expected that there was some absorption taking place in this experiment's frequency range. Although the reflections were most likely dampened, there were still reflections off all six directions: the sides, the ends, the bottom, and the air-water interface on the surface of the tank.

This experiment relies on the diffraction of sound around the balloon, and removing the reflections from the signal using gating became essential to provide conclusive proof that the introduction of the balloon decreased the received signal's amplitude. Gating uses a time series approach to analyzing a signal so that an operator can distinguish between the

direct path signal and any reflections that may be present. The tank's dimensions are 2.13 meters deep, 2.13 meters wide, and 6.40 meters long. The range of wavelengths was 30 centimeters to 3 meters, so these dimensions did not allow for enough difference in time for the direct path sound to be detected separate from the reflected sound. If the tow tank had been somewhat deeper, gating may have been feasible; as it was, the tow tank was not sufficiently large for conclusive data to be taken.

C. SLAMR FACILITY

The Sea Land and Air Military Research (SLAMR) facility located across a street from the NPS is the expected next step for this research project. The SLAMR Facility is an old wastewater treatment facility that has three large tanks that were used for aeration of wastewater. They have been cleaned and inspected, and are being repurposed for experimental and educational uses. All of the tanks are filled to the same level, and one of the tanks called AQE1, farthest from the ocean in Figure 27 is filled with treated water. The two tanks closest to the ocean, AQE2 and AQE3, are filled with untreated water. A common access trough runs unobstructed along the northeast edge. Each AQE holds approximately 415,000 gallons of water and is approximately 34.13 meters long, 11.28 meters wide, and a high-water level depth of approximately 4.27 meters. This larger tank is twice the depth and more than twice the width of the tow tank in the basement of Spanagel Hall. Therefore, it is expected that the reflections could be clearly differentiated from the direct path due to the extra distance that the reflections will have to travel in this tank compared to the tow tank. The use of the SLAMR facility will present a new set of challenges compared to the indoor tank. First, it is outside, so it is open to the elements and more sources of ambient noise. It is near the ocean so there will be a consistent amount of wind and ocean noise. It is also located close to a busy road, so there may be vibrations that are carried through the large amount of pavement to the concrete tank. Most of the equipment used is very expensive, so equipment will have to be transported to and from the basement of Spanagel in between test runs since it cannot be left outside due to weather damage or theft. This logistical problem can be solved in about a two-mile drive round trip from Spanagel to the SLAMR facility. This will be a tedious task since reconnecting all the equipment is a time-consuming and focus intensive process. It is very important to

ensure that all of the connections are correct because all of the equipment is very sensitive. Data collection at this location with the same procedure conducted previously will be an estimated four hours or more per task. The tank is twice as deep as the tow tank, and testing will most likely be conducted in the very center of the tank so that the reflections have to travel the maximum distance to get to the receiver. Therefore, the apparatus will be accessed via the catwalks that are above each tank, depicted in Figure 28. This will create the need for much longer cables and ropes to attach to the experimental apparatus to move the balloon suspension anchor, raise and lower the balloon, and connect the projecting and receiving hydrophones to the processing equipment. Extension cords will need to be used to get power all the way out to the tanks from an exterior outlet.

Screen capture of SLAMR Facility using satellite view from Google Maps. [7]

Figure 27. Overhead view of SLAMR facility tanks

Figure 28. Tank AQ1 with catwalk

D. TRANSDEC FACILITY

The Transducer Evaluation Center (TRANSDEC) in San Diego may be another option if the SLAMR is not sufficiently deep for testing displayed in Figure 29. This facility is located at the Naval Information Warfare Center Pacific (NIWC Pacific), formerly known as the Space and Naval Warfare Systems Center Pacific (SPAWAR Pacific) on Point Loma in Southern California. The TRANSDEC tank is the ultimate hydrophone testing facility due to the fact that it is elliptical with axes 300 feet and 200 feet and 38 feet deep with 6 million gallons of water [8]. The pool is anechoic and is designed specifically as a controlled environment with low ambient noise for transducer calibration and underwater acoustic facility. A similar logistical challenge is presented here with experimentation as the SLAMR facility with a more extreme trip of 439 miles and traveling with equipment. As well as having enough cabling and rope for the depth of the water.

Funding for travel and lodging will be required, so testing should be fully exhausted at the SLAMR facility before this is used to be more responsible with resources. There may also be costs associated with using this facility for testing.

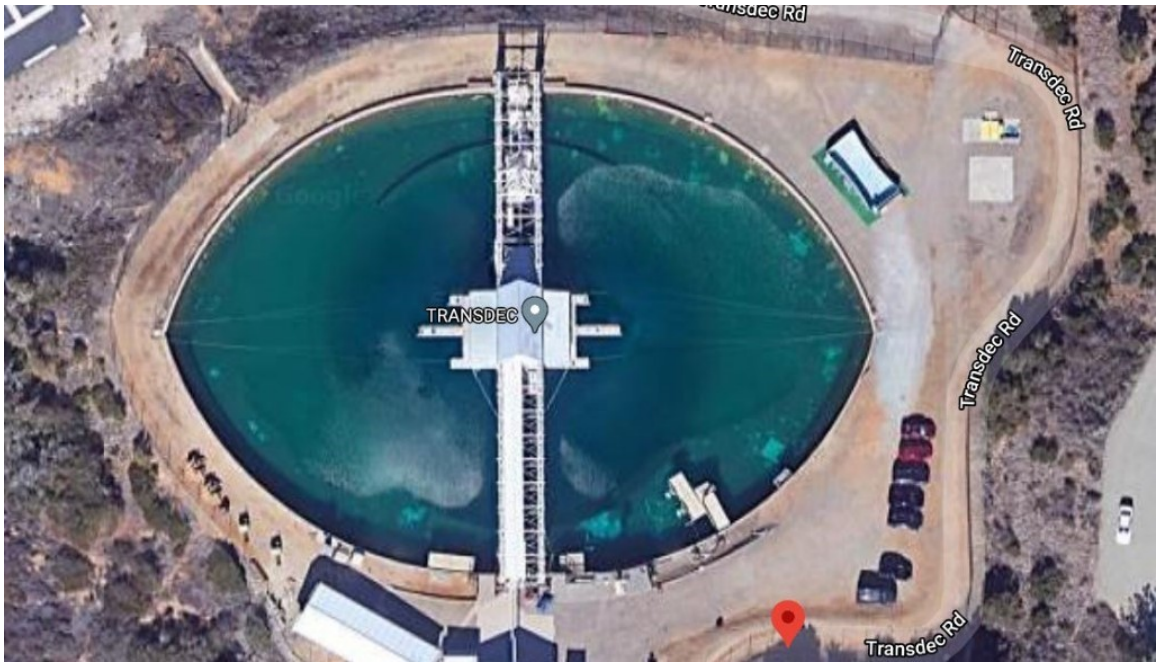

Screen capture of SLAMR Facility using satellite view from Google Maps. [9]

Figure 29. TRANSDEC facility satellite view

THIS PAGE INTENTIONALLY LEFT BLANK

APPENDIX. ADDITIONAL THEORETICAL GRAPHS

A. DESCRIPTION

The following sections show theoretical graphs for more realistic values of the parameters than those used in Sec. III.B to compare to the experiment. In that section, a soft sphere with no mass (M = 0) and no dissipation is assumed. For comparison, the theoretical graphs of the section are included in this appendix. For the strong dissipation, the imaginary part of the speed of sound is taken to be 1% of the real part.

The conclusion from the graphs in this appendix is that the ratio of the theoretical amplitudes plotted in Sec. III.B are only weakly affected by the fluid in the sphere, for the parameters and frequency range of the experiment. This justifies the assumption of a soft sphere with no dissipation.

B. 0-DEGREES CONFIGURATION

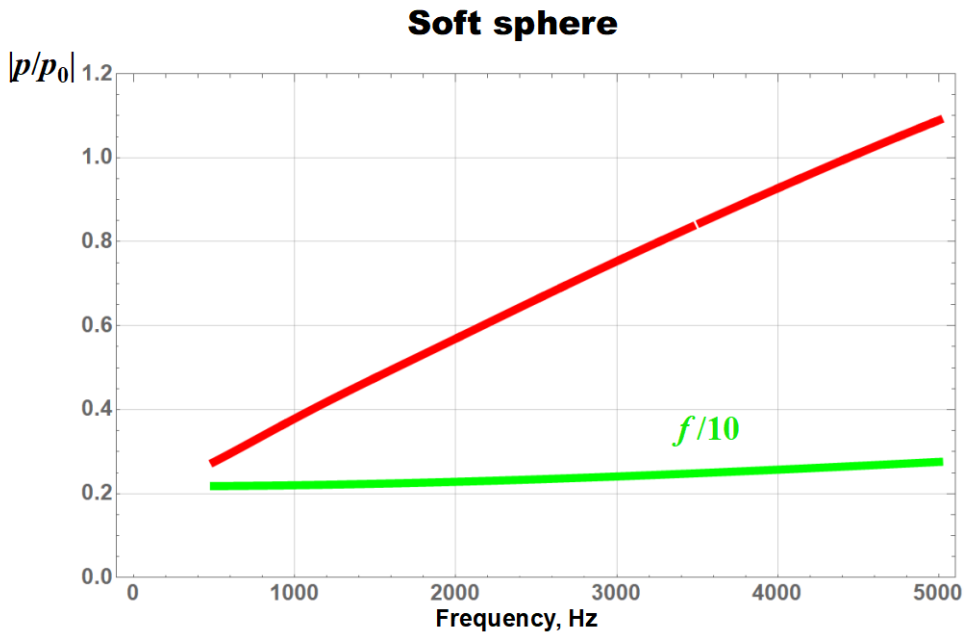

Figure 30. Perfect pressure release boundary assumption

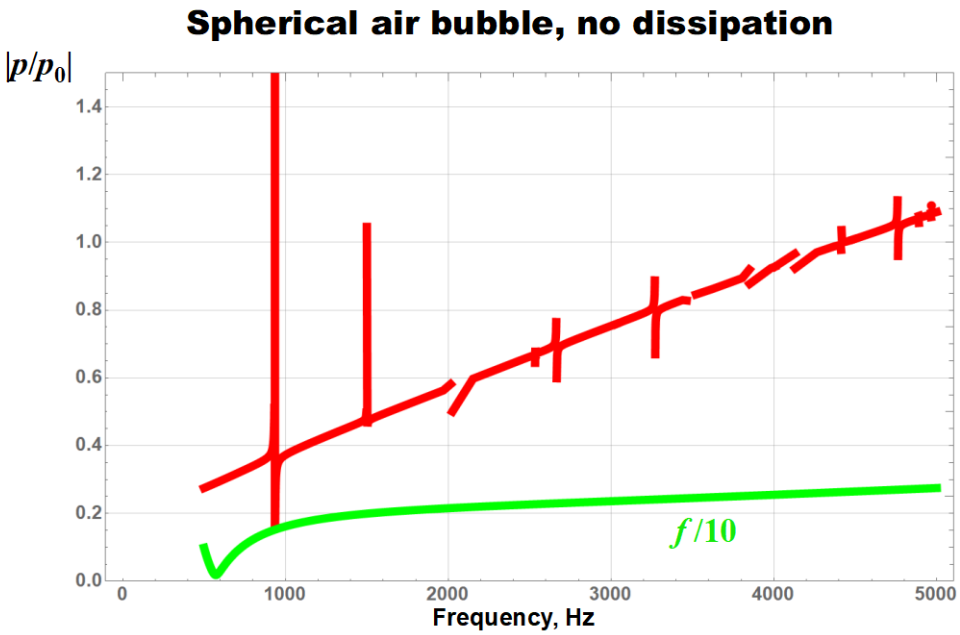

Figure 31. Spherical air bubble without absorption in air

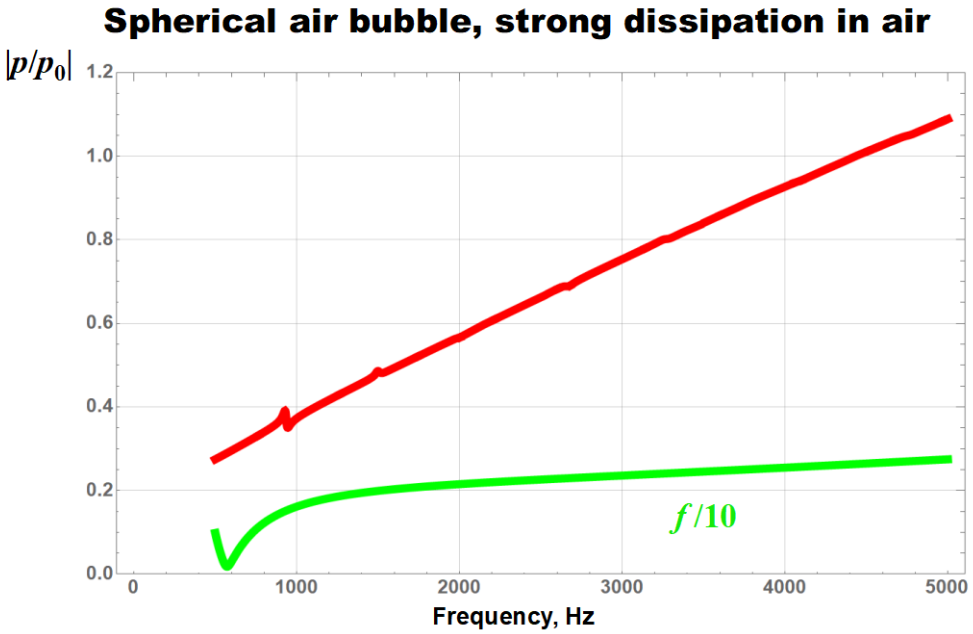

Figure 32. Spherical air bubble with strong absorption in air

C. 90-DEGREES OR 270-DEGREES CONFIGURATION

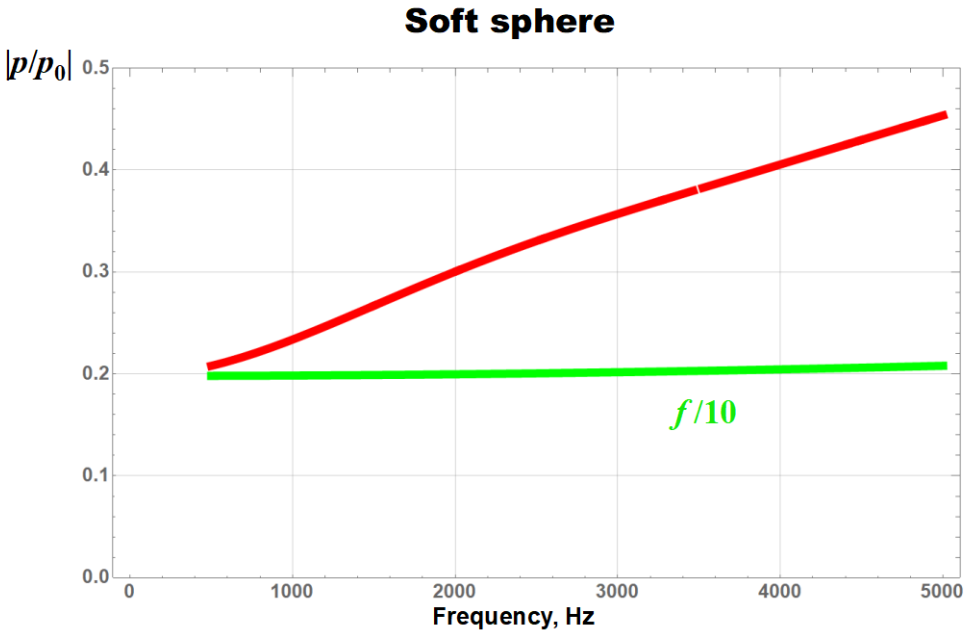

Figure 33. Perfect pressure release boundary assumption

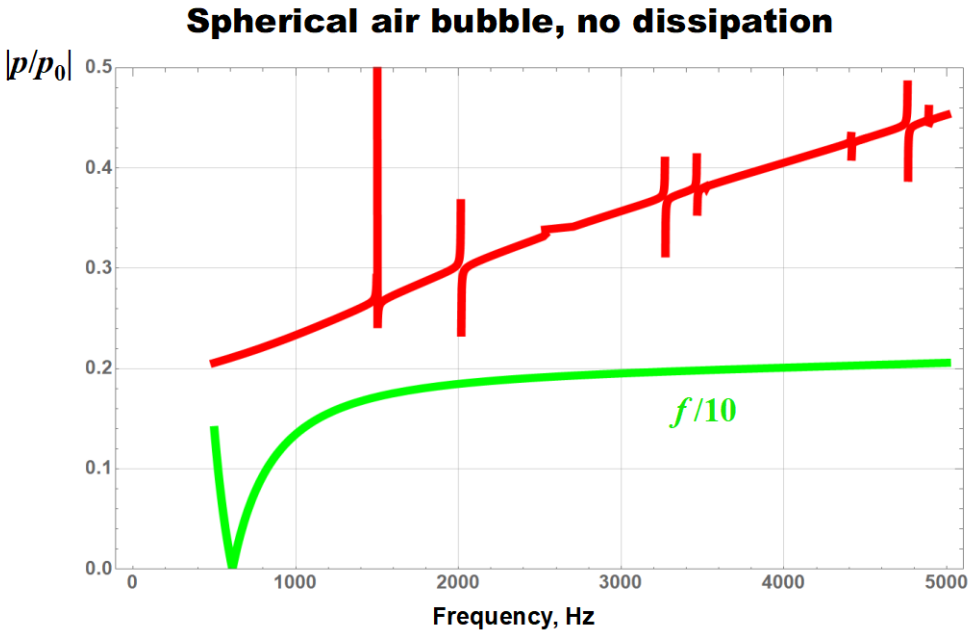

Figure 34. Spherical air bubble without absorption in air

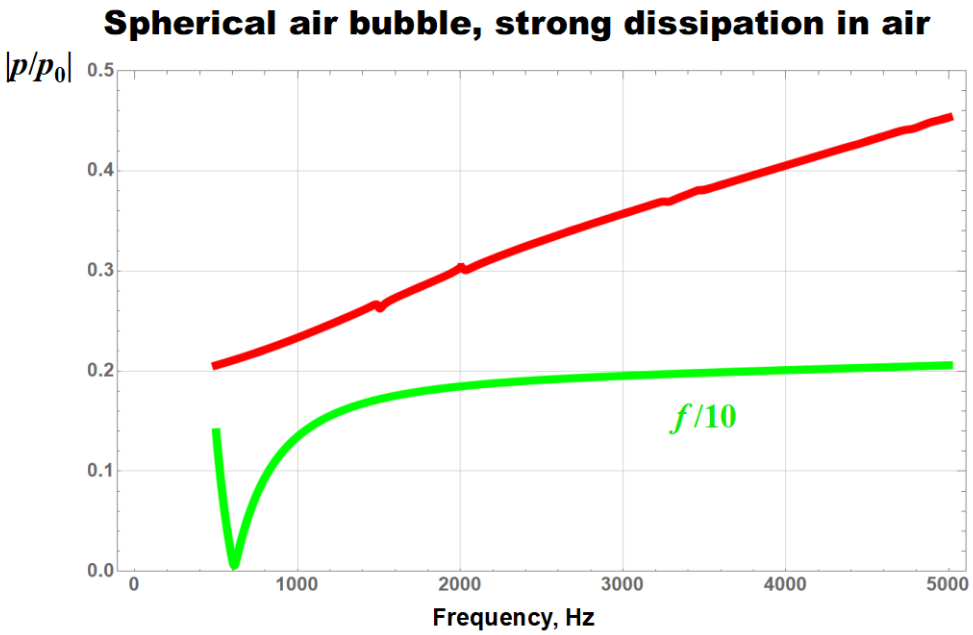

Figure 35. Spherical air bubble with strong absorption in air

D. 180-DEGREES CONFIGURATION

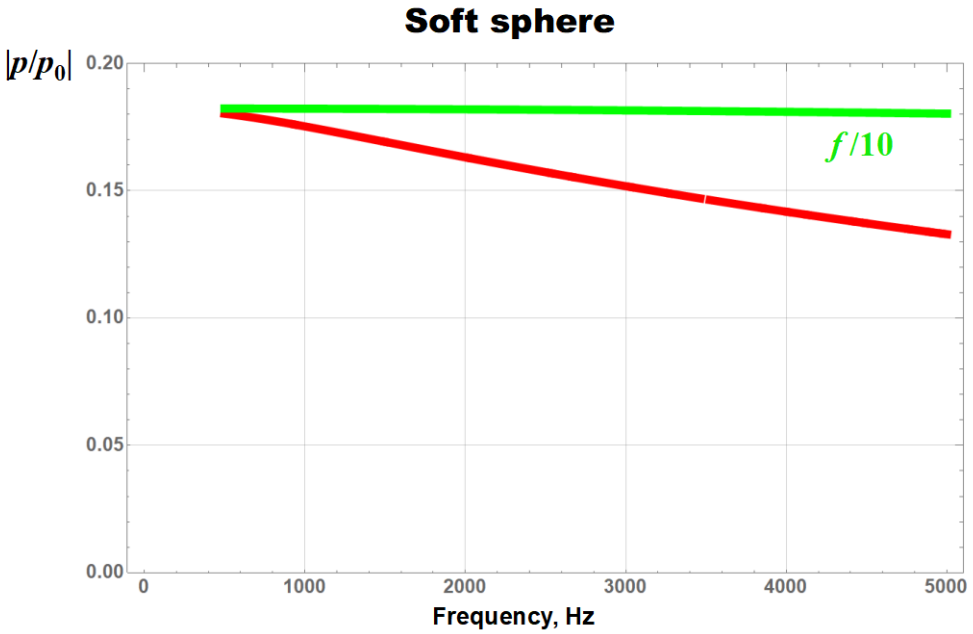

Figure 36. Perfect pressure release boundary assumption

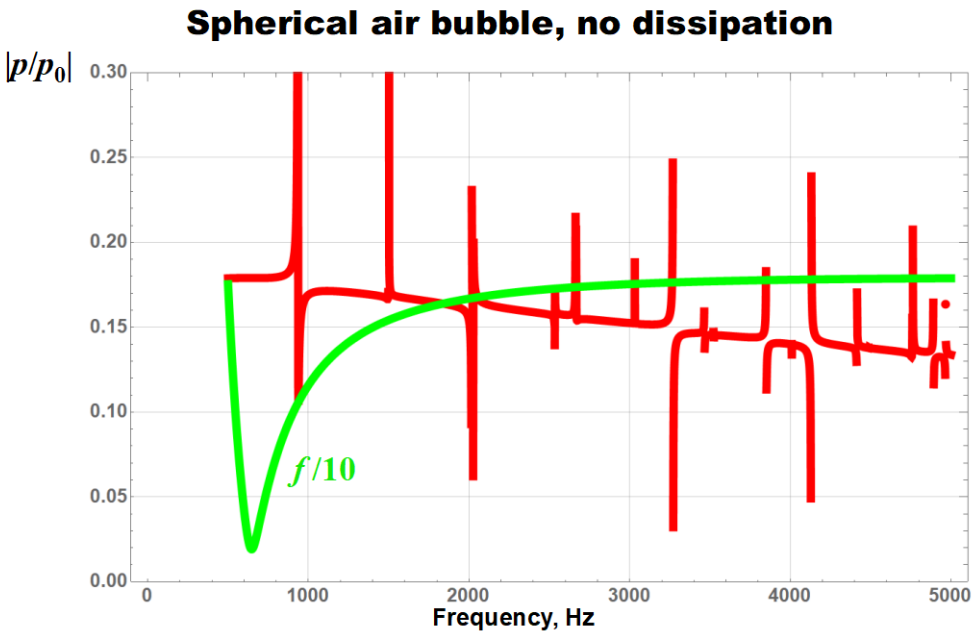

Figure 37. Spherical air bubble without absorption in air

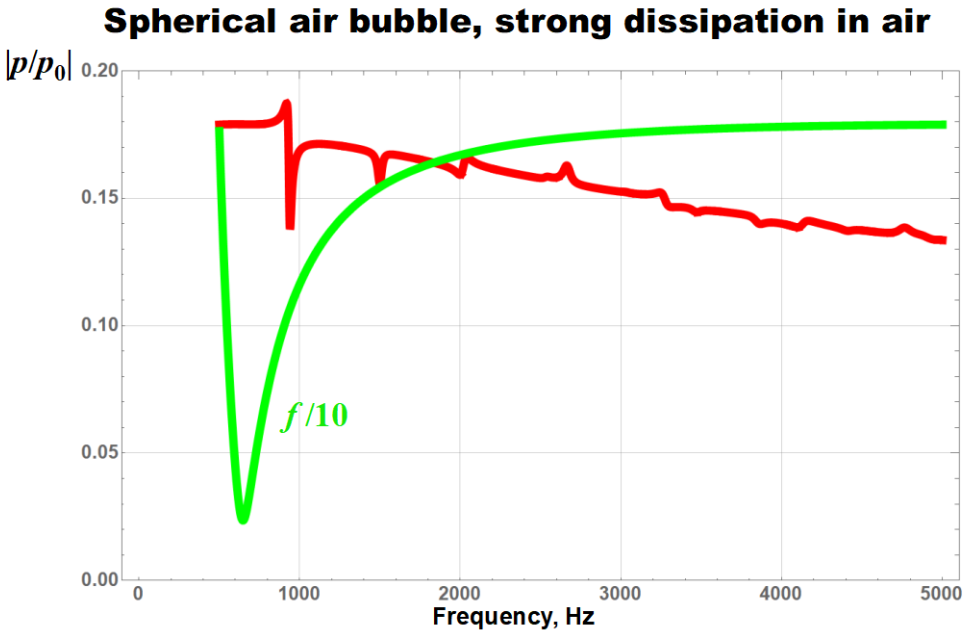

Figure 38. Spherical air bubble with strong absorption in air

THIS PAGE INTENTIONALLY LEFT BLANK

LIST OF REFERENCES

[1] W. J. Richardson, C. R. Greene, Jr., C. I. Malme, and D. H. Thomson, *Marine Mammals and Noise.* San Diego: Academic Press, 2013.

[2] B. Würsig, C. R. Greene, Jr., and T. A. Jefferson, "Development of an air bubble curtain to reduce underwater noise of percussive piling," *Mar. Environ. Res*. vol. 49, p. 79–93 (2000).

[3] O. A. Godin and A. B. Baynes, "Passive, broadband suppression of low-frequency sound," *J. Acoust. Soc. of America*, vol. 143, no. 2, p. 67-73, January 2018.

[4] J. Lee, K. Lee, H. Park, and J. Kim, "Possibility of air-filled rubber membrane for reducing hull exciting pressure induced by propeller cavitation," *Ocean Engineering,* vol. 103, p. 160–170, July 2015.

[5] J. J. Murawski, "Use of bubbles for pressure minesweeping," M.S. thesis, Dept. of Eng. Acoustics, NPS, Monterey, CA, 2009.

[6] Dassault Systemes, SolidWorks. [Download]. Waltham, MA: Dassault Systemes SolidWorks Corporation, 2019.

[7] Google. "NPS SLAMR facility." Nov, 8 2020. [Online]. Available: https://www.google.com/maps/place/Naval+Postgraduate+School/@36.6026141,-121.8720357,312a,35y,339.47h,4.15t/data=!3m1!1e3!4m5!3m4!1s0x808e00e558298b37:0x972fe8117718bc7!8m2!3d36.5971756!4d-121.8740833.

[8] Wikimapia, "TRANSDEC anechoic pool." Nov. 8 2020. [Online]. Available: http://wikimapia.org/1362997/TRANSDEC-Anechoic-Pool

[9] Google. "TRANSDEC facility." Nov, 8 2020. [Online]. Available: https://www.google.com/maps/search/transdec+facility/@32.703417,-117.2504948,87m/data=!3m1!1e3.

THIS PAGE INTENTIONALLY LEFT BLANK

INITIAL DISTRIBUTION LIST

1. Defense Technical Information Center
   Ft. Belvoir, Virginia

2. Dudley Knox Library
   Naval Postgraduate School
   Monterey, California